THE UNIVERSITY of ADELAIDE

WORKING PAPER 26
CHANTHAVONG, OTCHIA

Critical minerals, critical choices: Reshaping EU strategy in global electric vehicle supply chains

Institute for International Trade

GROUP OF EIGHT AUSTRALIA

make history.

Critical minerals, critical choices: Reshaping EU strategy in global electric vehicle supply chains

About the authors

Sinthavanh Chanthavong is a Ph.D. candidate in International Development (Development Economics) at Nagoya University. His research focuses on the economic impacts of trade and industrial policies in Lao PDR, specifically analysing trade liberalization and market access using causal inference techniques and firm- and household-level data. Prior to his doctoral studies, Sinthavanh was a Trade Officer at the Ministry of Industry and Commerce, Lao PDR (2018-2022). In this role, he was a key technical official conducting comprehensive economic and legal assessments for the negotiation and national endorsement of major free trade agreements, specifically the ASEAN Agreement on Electronic Commerce and the Regional Comprehensive Economic Partnership (RCEP).

Dr. Christian Otchia is an Associate Professor of Development Economics at Nagoya University's Graduate School of International Development. His research focuses on industrial policy, trade integration, and structural transformation, employing Computable General Equilibrium (CGE) models and applied econometrics to analyse regional value chains and labour economics. He has served as Principal Investigator for multiple JSPS-funded research projects, including studies on intraregional trade in Central Africa and pro-poor industrial policy. Dr. Otchia has published extensively on topics such as private investment growth in Africa, special economic zones, and productivity in Ethiopian industrial parks.

Co-funded by the European Union

Abstract

This study examines the structural transformation of the global automotive industry driven by the transition to electric vehicles (EVs). By applying network analysis and Temporal Exponential Random Graph Models (TERGM) to bilateral trade data from 1995–2023, the research compares the evolution of traditional versus EV-oriented global value chains (GVCs). The analysis distinguishes a mature, regionally integrated traditional automotive network from an emerging EV configuration characterized by significant midstream concentration. In this structure, diffuse upstream raw material trade converges into a highly centralized processing and component manufacturing hub before diversifying again in finished vehicles. Econometric estimates indicate that these networks are governed by strong path dependence, reciprocity, and triadic closure, yet remain responsive to policy variables. Specifically, trade agreements are associated with network expansion, while tariffs correlate with reduced trade volume and fewer commercial ties, particularly in EV-related sectors. These findings highlight a policy tension for the European Union: the need to mitigate exposure to concentrated supply vulnerabilities while maintaining the open trade architecture required for a cost-effective green transition.

1. Introduction

The global automotive industry is in the midst of its most profound transformation in a century. The convergence of rapid technological disruption, escalating geopolitical competition, and ambitious climate policy has created a new industrial paradigm, fundamentally reshaping the structure of global production and trade. At the heart of this shift is the transition to electric vehicles (EVs), a market that has expanded at an unprecedented rate, with global sales surging from just 4% of the market in 2020 to 18% in 2023. This transition is not merely a substitution of one powertrain for another; it represents a fundamental re-architecting of global value chains (GVCs), shifting the locus of value from traditional mechanical engineering to battery technology, software, and the control of critical mineral supply lines.

This industrial metamorphosis is unfolding on a complex and contested global stage. Major economic blocs are pursuing divergent and often conflicting strategies to secure competitive advantage. The European Union, through its Critical Raw Materials Act, is attempting to build secure and sustainable supply chains to fuel its green transition. In contrast, the United States has vacillated between the protectionist, tariff-driven policies of the Trump administration, which introduced lasting fragmentation into global trade networks, and the subsidy-led industrial policy of the Biden administration's Inflation Reduction Act. Simultaneously, the EU's Carbon Border Adjustment Mechanism (CBAM) introduces a novel instrument at the nexus of trade and climate policy, creating price differentials based on carbon intensity and establishing a "green premium" that directly influences sourcing and investment decisions. These dynamics have magnified the risk of carbon leakage, a long-standing concern in environmental economics and a critical challenge for the effectiveness of EU climate policy.

Against this backdrop, the geography of the automotive GVC is being redrawn. African nations, particularly the Democratic Republic of Congo (home to 70% of global cobalt reserves) and South Africa (a key source of platinum group metals), have emerged as critical nodes in the upstream supply chain. The Asia-Pacific region plays an equally vital, albeit more complex, role. Chinese state-led investment in both African mineral extraction and downstream manufacturing in ASEAN nations has created intricate trilateral dynamics that directly shape the EU's strategic options.

A substantial literature examines the technological, geopolitical and policy aspects of the EV transition, but these strands are often treated separately and only occasionally linked to a trade-network perspective. As a result, evidence on how these forces jointly relate to changes in the structure of automotive production and trade remains limited. This paper offers an exploratory contribution by using network analysis, TERGMs and gravity models on bilateral trade data to examine how the EV transition is reflected in automotive and EV-related trade networks, and to discuss what this may imply for European Union's evolving industrial and climate-trade policies in light of its exposure to concentration in selected segments of the supply chain. In this paper, we combine exploratory network analysis of automotive and EV trade with Temporal Exponential Random Graph Models and gravity estimations that incorporate standard economic, geographic and trade-policy covariates.

This research is situated at the intersection of three converging literature streams: Global Value Chain (GVC) structures, the technological and geopolitical dimensions of the EV transition, and trade policy instruments. First, the foundational literature on GVCs provides the analytical lens for understanding the structure of international production. The automotive industry, in particular, has been characterized by highly regionalised, "nested" GVCs, a structure dictated by high capital costs, the technical demands of just-in-time production, and political pressures for local content (Sturgeon et al., 2008). This regionalism is embedded within a deeper, long-term core-periphery structure in global trade that has proven remarkably stable over decades, with only a few countries achieving upward mobility (Mahutga, 2006). Network analyses of trade data have empirically confirmed this architecture, revealing a "twin dynamic" of deepening regionalisation around industrial hubs in Europe (Germany) and North America (the US), alongside growing cross-regional integration driven by the rise of new industrial powers like China and Mexico (Russo et al., 2022). This structure, however, is not monolithic; disaggregated analyses show that trade networks for different components, such as engines versus electrical parts, evolve with distinct topologies (Gorgoni et al., 2018). Despite this robust architectural mapping, there remains room to explore how policy shocks propagate through these networks over time.

Second, scholarship on the technological and geopolitical dimensions of the EV transition highlights the depth of the industrial shift. The transition is more than a change in powertrain; it is a redefinition of the industry into a data-driven mobility sector, making it a central battleground in the broader technological competition between the US, EU, and China (Ciuriak, 2025). This technological revolution is, in turn, critically dependent on a secure and reliable supply of raw materials such as lithium, cobalt, and rare earth elements. This dependency has ignited a global geopolitical "race for critical minerals," as nations and firms scramble to secure upstream resources in an era of great power competition (Kalantzakos, 2020). The resulting supply chains are fraught with vulnerabilities. The global trade network for Li-ion batteries, for instance, has a "robust-yet-fragile" structure where disruptions at key nodes like China or South Korea can trigger significant risk transmission (Hu et al., 2021). Similarly, the trade in rare earths is characterized by a stable dependence of resource-scarce countries on a few resource-rich ones (Yu et al., 2022). While key drivers are identified, this leaves an opportunity to model how mineral risks interact dynamically with trade policy shifts.

Third, the literature on climate and trade policy has analysed the potential impacts of the new and increasingly contentious instruments governing global trade. Geopolitical friction, exemplified by the

US-China trade war, has been shown to create pervasive uncertainty that directly hinders corporate investment in green innovation (Cao and Hu, 2025). Simultaneously, the EU's CBAM represents a pivotal new instrument designed to prevent carbon leakage by levelling the playing field between domestic and foreign producers (Erdogdu, 2025), (Pan and Liu, 2024). Retrospective analysis of the EU's Emissions Trading System (ETS) confirms that the risk of carbon leakage is significant, underscoring the need for a carefully designed border adjustment (Böning et al., 2023). While the aggregate economic impact of the CBAM may be modest, analyses show that the costs can be substantial for specific carbon-intensive products and may disproportionately affect developing countries, explaining its political salience (Dolphin and Ferrucci, 2025). These studies clarify policy effects, opening a path to investigate how trade instruments shape EV-driven GVC restructuring.

In synthesizing these streams, our research contributes by bridging these interconnected gaps. While prior work has provided foundational GVC analysis (Sturgeon et al., 2008, Russo et al., 2022), modelled component networks (Hu et al., 2021), or assessed trade policy impacts, few studies combine EV technology, mineral supply context, and trade policy instruments within a unified network evolution model. This paper seeks to advance this agenda by offering an empirical analysis of recent transformations in the automotive GVC. By employing Temporal Exponential Random Graph Models (TERGM) (Leifeld et al., 2018), we examine how these factors are associated with changes in the structure of international automotive trade networks over time, providing a more integrated perspective on the forces reshaping the global industry.

The remainder of this paper is organized as follows. Section 2 outlines data and methods. Section 3 maps the evolving automotive and EV network structures, identifying concentrated midstream chokepoints. Section 4 employs TERGM and gravity models to quantify trade drivers and network dynamics. Finally, Section 5 discusses the broader policy implications for the European Union, alongside study limitations and directions for future research.

2. Data and methodology

This research employs a multi-stage quantitative methodology designed to empirically model the structural transformation of the automotive value chain.

2.1. Data

Our analysis relies on a comprehensive panel dataset constructed from multiple sources, covering global bilateral trade and policy data from 1995 to 2023.

Trade data: This study draws on bilateral trade data at the HS 6-digit level from the CEPII BACI database, which is widely recognized for its rigorous harmonization process that reconciles mirror flows to ensure consistency and accuracy in global trade statistics (Gaulier and Zignago, 2008). To analyse the automotive sector, we classify products into value-chain-based categories using the HS nomenclature, building on the automotive value chain framework proposed by Sanon and Slany (2023) and the electric vehicle (EV) value chain outlined by UNCTAD (2023). Under the Harmonized System (HS), the automotive industry falls primarily within Section XVII (Transport Equipment) and is specifically detailed in Chapter 87 (Vehicles and Parts). Within the HS 1992 nomenclature, automotive products are organized into three tiers: (i) finished vehicles, (ii) parts and components, and (iii) raw and semi-processed materials. In HS 2017, the classification is refined to capture the technological complexity of electric vehicles (EVs). EV-related products are disaggregated into six categories: (i) battery materials, (ii) core EV components and electronics, (iii) raw minerals, (iv) processed minerals, (v) finished electric vehicles, and (vi) charging and infrastructure equipment. A detailed list of the HS codes corresponding to each category is provided in the Appendix. This distinction between HS versions provides a systematic basis for analysing trade flows across conventional automotive and EV supply chains, linking upstream resource extraction to downstream assembly and market integration.

Trade policy data: We use the Teti (2024)'s Global Bilateral Tariff Dataset, which harmonizes applied and MFN tariff rates across countries and years by systematically addressing missing, inconsistent, and unreported observations. This dataset integrates and improves upon primary sources such as UNCTAD TRAINS, WTO IDB, and ITC MACMAP, providing bilateral tariff data at both HS section and country-pair levels. To capture structural and policy determinants, we incorporate country-level variables from the CEPII Gravity Database (Conte et al., 2022) and (Gurevich, 2018), including economic size, geography, and institutional characteristics. Since the gravity dataset covers up to 2021 while our trade data extends to 2023, we update macroeconomic indicators using the World Bank WDI and complement trade policy variables with the Regional Trade Agreements (RTA) Database (Larch, 2020). All datasets are harmonized using ISO3 codes and merged into a balanced panel, ensuring consistency across trade, tariff, and gravity dimensions.

2.2 Analytical framework

Exploratory network analysis

We adopt a social network analysis approach to represent global trade as a directed and weighted network where economies are nodes and bilateral trade flows are edges. Social network analysis provides a formal framework for studying relational structures and measuring properties such as density, centrality, and clustering, which are essential for understanding systemic interdependencies (Wasserman, 1994). Building on this theoretical foundation, recent methodological advances emphasize practical applications of these techniques, including visualization, descriptive metrics, and inferential models for dynamic networks (Yang et al., 2016) Applied to international trade, this approach allows researchers to capture the topology of the global trade system, identify hubs and communities, and analyse structural changes over time (De Benedictis et al., 2014). In this study, we construct abstract networks of trade in the automotive sectors, including non-EV and EV value-tier flows based on the determined classification. The graphs are constructed with the "igraph" package in R by (Csardi and Nepusz, 2006) using the Fruchterman–Reingold Force-Directed layout, where nodes are positioned through an iterative force-directed algorithm that simulates repulsive forces between nodes and attractive forces along edges, resulting in a balanced and visually interpretable layout where connected nodes are closer together (Fruchterman and Reingold, 1991). A simple backbone extraction is applied by filtering the most significant trade flows and removing noise from less relevant transactions. We then compute measures that capture connectivity, clustering, and community structure, providing insights into the evolution of automotive trade networks over recent decades.

Network modeling

To analyse the evolution of the automotive industry trade landscape, we employ a Temporal Exponential Random Graph Model (TERGM). This statistical framework is designed to model the dynamic formation and persistence of network ties over time. The TERGM is a longitudinal extension of the Exponential Random Graph Model (ERGM), which models a network's global topology as a function of its local configurations (Wasserman, 1994). ERGMs explain network structure through endogenous dependencies, such as reciprocity and triadic closure, as well as exogenous dyadic and nodal attributes. However, standard ERGMs are specified for cross-sectional data and thus cannot account for the strong temporal dependence and inertia inherent in international trade networks. TERGMs address this limitation by explicitly modelling the evolution of the network, conditioning the current state on its past

configurations (Hanneke et al., 2010). Recent applications in trade research underscore the model's utility. For example, (Ding et al., 2025) utilizes a TERGM to show that an agricultural trade network evolved into a "core–edge" structure, driven by endogenous reciprocity and network expansion. Their findings indicate that while geographical proximity and cultural similarity reduced transaction costs, distance remained a key constraint. Similarly, (Feng et al., 2024) finds that the global renewable energy trade network expanded into a small-world structure with strong reciprocity and community clustering, where dominant hubs emerged and ties were heavily influenced by regional agreements. These studies demonstrate the capacity of TERGM to analyse structural evolution and the impact of policy shocks within global value chains.

Our approach integrates a network perspective with the established gravity model of trade. The gravity model, specified in its standard multiplicative form to accommodate zero trade flows and heteroscedasticity Silva and Tenreyro (2006) provides the theoretical foundation for our covariate selection. Following the specification proposed by (Larch and Yotov, 2024), the model is expressed as:

$$\boldsymbol{T}_{ij,t} = \exp\left(\boldsymbol{\gamma}'\boldsymbol{G}_{ij,t} + \boldsymbol{\delta}'\boldsymbol{D}_{ij} + \boldsymbol{\rho}'\boldsymbol{P}_{ij,t} + \boldsymbol{\alpha}_{ij} + \boldsymbol{\phi}_{i,t} + \boldsymbol{\psi}_{j,t}\right) \times \boldsymbol{\epsilon}_{ij,t} \quad (1)$$

Here, the trade flow $\boldsymbol{T}_{ij,t}$ is a function of nodal gravity variables $\boldsymbol{G}_{ij,t}$, including GDP and population; dyadic gravity variables $\boldsymbol{D}_{ij}$, such as distance and contiguity, and dyadic policy variables $\boldsymbol{P}_{ij,t}$, like trade agreements and tariffs. The terms $\boldsymbol{\alpha}_{ij}$ (pair or directional pair), $\boldsymbol{\phi}_{i,t}$ (exporter-time), and $\boldsymbol{\psi}_{j,t}$ (importer-time) are fixed effect terms that control for unobserved time-invariant and time-varying multilateral resistance. Extending this framework, we formally define the Temporal Exponential Random Graph Model (TERGM) as a probabilistic model in which the likelihood of observing a network state $\boldsymbol{N}_t$is explicitly conditioned on its historical configurations, as well as nodal and edge-level covariates. The general specification of the model is given by:

$$\boldsymbol{P}\left(\boldsymbol{N}_t \mid \boldsymbol{N}_{t\text{-}1}, \ldots, \boldsymbol{N}_{t\text{-}K}, \boldsymbol{\theta}\right) = \frac{\exp\left(\boldsymbol{\theta}^T \boldsymbol{h}\left(\boldsymbol{N}_t, \boldsymbol{N}_{t\text{-}1}, \ldots, \boldsymbol{N}_{t\text{-}K}\right)\right)}{\boldsymbol{c}\left(\boldsymbol{\theta}, \boldsymbol{N}_{t\text{-}1}, \ldots, \boldsymbol{N}_{t\text{-}K}\right)} \quad (2)$$

Equation (2) formalizes the TERGM as a probabilistic framework for network evolution, defining the conditional probability of observing a specific network structure at time given its history. The model $\boldsymbol{P}\left(\boldsymbol{N}_t \mid \boldsymbol{N}_{t\text{-}1}, \ldots, \boldsymbol{N}_{t\text{-}K}, \boldsymbol{\theta}\right)$ operates under a k-order Markov assumption, meaning the current network state $\boldsymbol{N}_t$depends on its configurations over the past $\boldsymbol{K}$ periods. The numerator, $\left(\boldsymbol{\theta}^T \boldsymbol{h}\left(\boldsymbol{N}_t, \boldsymbol{N}_{t\text{-}1}, \ldots, \boldsymbol{N}_{t\text{-}K}\right)\right)$, contains the core specification, where $\boldsymbol{h}$ is a vector of network statistics that count endogenous configurations, exogenous covariate effects drawn from the gravity-based matrices $\boldsymbol{G}_{ij,t}$, $\boldsymbol{D}_{ij,t}$, and $\boldsymbol{P}_{ij,t}$, and crucial temporal dependencies (e.g. the persistence of ties from $\boldsymbol{N}_{t\text{-}1}$ to $\boldsymbol{N}_t$). Each statistic in this vector is weighted by a corresponding parameter in $\boldsymbol{\theta}^T$, which quantifies its influence on the log-odds of tie formation.

The denominator $\boldsymbol{c}\left(\boldsymbol{\theta}, \boldsymbol{N}_{t\text{-}1}, \ldots, \boldsymbol{N}_{t\text{-}K}\right)$ represents a normalizing constant that ensures the model defines a proper probability distribution by summing the numerator over the entire space of possible network configurations. Due to the combinatorial complexity of this term, exact computation is infeasible for large-scale networks. Accordingly, parameter estimation relies on approximation techniques. Given the high dimensionality and sparsity of the network under study, we employ Maximum Pseudolikelihood Estimation (MPLE), which provides a computationally tractable alternative to full likelihood methods such as Markov Chain Monte Carlo Maximum Likelihood Estimation (MCMC-MLE). Estimation is implemented using the `btergm` package in R, which applies a bootstrapped MPLE procedure tailored for the graph models in large network settings (Leifeld et al., 2018).

3. Exploratory networks analysis

This section presents the results of our exploratory analysis, which maps the evolving architecture of the automotive Global Value Chain (GVC). The analysis was conducted in R using the 'igraph' package to construct network objects from bilateral trade data and calculate key network- and node-level metrics.

To focus the analysis on the structural backbone of the trade network and ensure robust visualization, a simple filtering technique was applied: only the top 0.5 or 1 percentile of bilateral trade values per period were retained. This filtered network was then used for abstract visual graph analysis and subsequent metric calculation. The analysis proceeds by first assessing macro-level trends in density and resilience, then examining the shifting global topology and regional hierarchies, and finally contrasting the traditional automotive structures with the emergent Electric Vehicle (EV) paradigm.

3.1. Evaluation of automotive trade networks

The overall automotive trade network has undergone a significant transformation since 1995, evolving from a sparser, more centralized system into a denser, more multipolar, and deeply integrated global production system. This structural evolution is clearly visible in the network graphs presented in Figure 1, which depict the GVC at four distinct time intervals. The quantitative trends underpinning this visual transformation are detailed in Figure 1, which plots the evolution of key network metrics over time. The graphs clearly show the steady growth in the number of participating economies (nodes) and a more dramatic increase in trade relationships (edges), which together drive the rise in network density. The total value of trade also shows a consistent upward trend, punctuated by sharp but temporary declines corresponding to major economic shocks.

The network metrics for global automotive trade (HS Chapter 87) from 1995 to 2023 provide a dynamic, empirical confirmation of the GVC's unique architecture. The foundational literature has long characterized this industry as being defined by highly regionalised, "nested" value chains (Sturgeon et al., 2008), which are themselves embedded within a stable, long-term "core-periphery" global structure (Mahutga, 2006). Our longitudinal data strongly supports this dual characterization, revealing a system that has become simultaneously more interconnected yet rigidly hierarchical. This structural rigidity is most clearly quantified by the Degree Assortativity, which remains consistently negative throughout the observation period. In network science, negative assortativity serves as a statistical proxy for structural dependency. It indicates that peripheral economies rarely form trade links with one another but instead attach preferentially to core industrial powers. Furthermore, the evolution of local structure validates the "twin dynamic" of globalization identified by Russo et al. (2022), defined by the simultaneous deepening of regional blocs and the integration of those blocs into a global system. The steady rise in the Global Clustering Coefficient provides empirical evidence of "deepening regionalisation," a state where trading partners increasingly form tight, triangular production cells to support just-in-time manufacturing. Conversely, the persistently high Eigenvector Centrality Gini reflects "growing cross-regional integration" orchestrated by a select few dominant nodes. Together, these metrics depict an industry where efficiency is achieved through regional densification, yet strategic influence remains centralized in the traditional core.

A critical, under explored question is the resilience of this system to sharp shocks. Our time-series data offers direct findings. The network endured two massive contractions during the 2008-2009 Global Financial Crisis and the 2019-2020 COVID-19 pandemic. Despite this volatility, core structural metrics such as global clustering and reciprocity remained remarkably stable. Evidence favours diversion and reconfiguration of flows over true fragmentation, reflecting high structural resilience. This efficiency is also seen in the weighted average path length, which plummeted over the period, making the network far more integrated.

These global structural trends are visually confirmed by the network topology graphs in Figure 2, which show the persistent dominance of a few core hubs. As the 1995-1999 graph shows, the initial structure is a clear core-periphery model, dominated by the United States (USA), Germany (DEU), and Japan (JPN). This core dominance by the US and Germany remains an "essential" feature across all four periods. The topology itself delineates their specific strategic functions: the United States consistently occupies the central bridging position of a primary broker while Germany displays the dense radial connections of a central organizer. This visual configuration confirms their enduring roles as the gravitational centres of the North American and European GVCs respectively.

Figure 1: Evolution of key automotive trade network metrics (1995-2023)

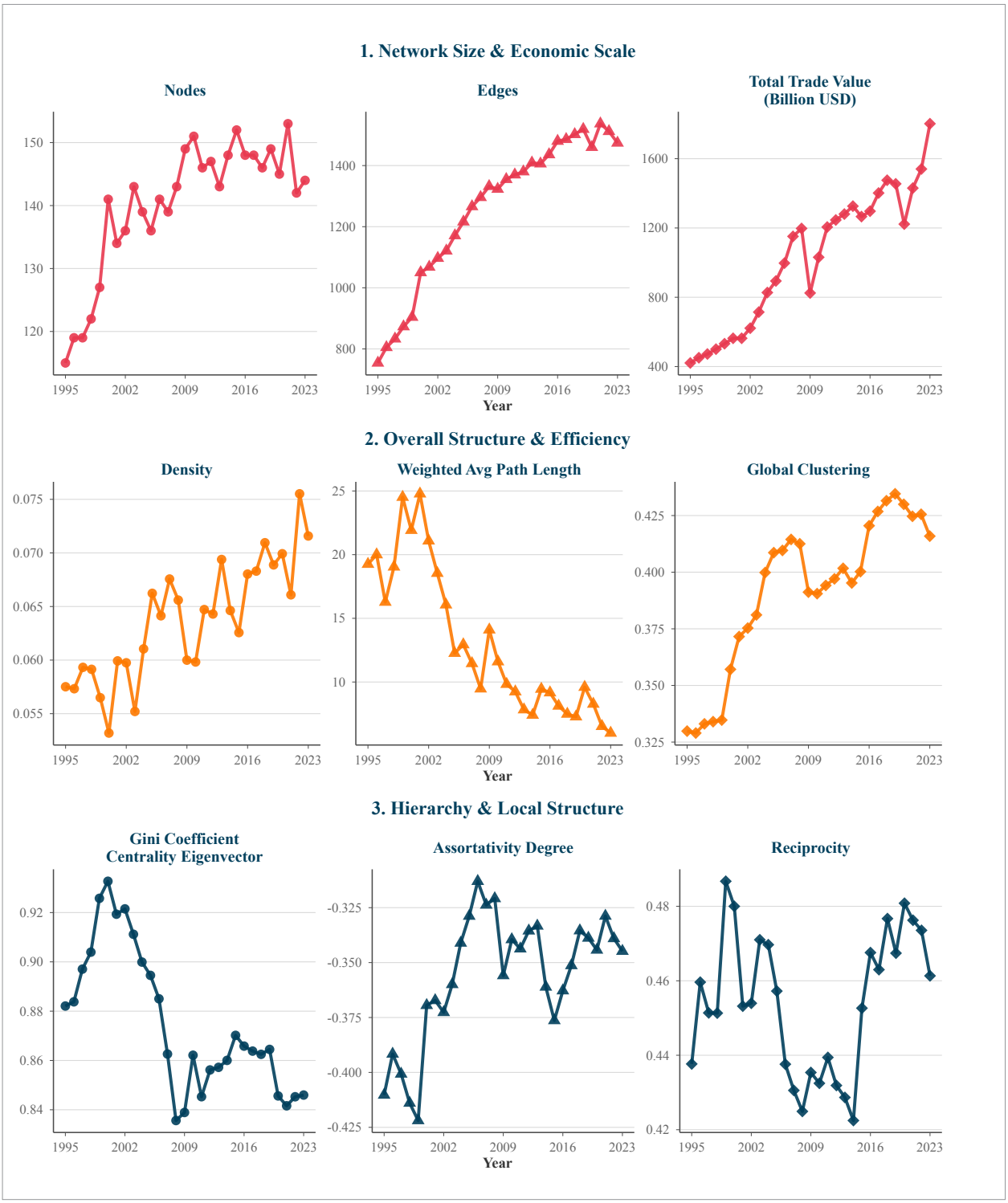

Note: This network matrix was calculated using the igraph package. We set the threshold at 10 percent to filter out the noise from the network.

Figure 2: Structural shifts in sutomotive trade networks (1995–2023)

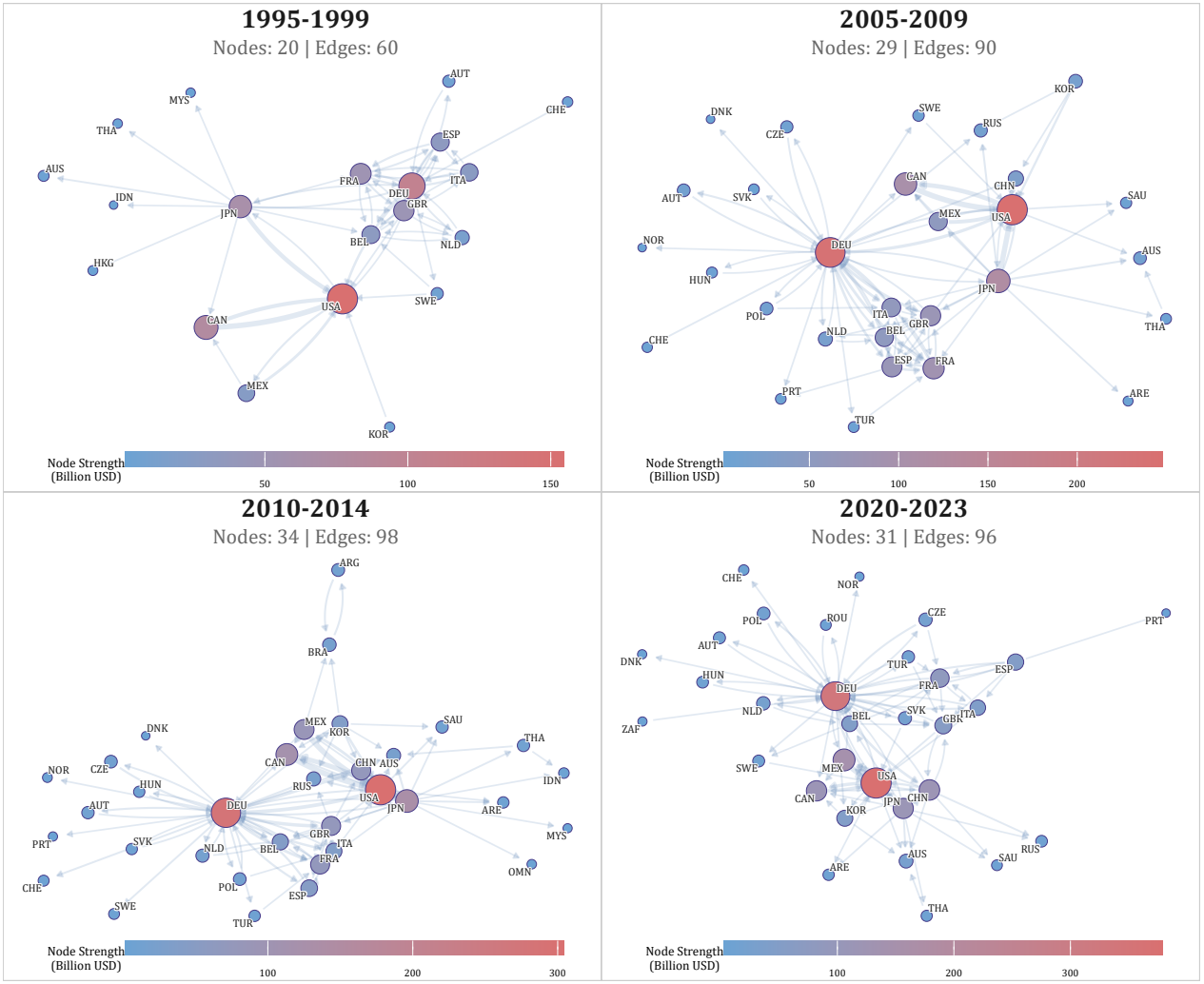

Note: The graph visualizes export data from HS Chapter 87 (Vehicles and Parts), covering automotive products and equipment. The threshold was set at the top 0.5 percentile to suppress minor flows and highlight the structural backbone of the global trade network. Crucially, the filtering was applied independently within each time bin.

The network graphs also visualize the significant “big shift” in the North American production bloc, particularly after the year 2000. While the 1995-1999 graph shows a less connected structure, the 2005-2009 graph and those following clearly illustrate the deep integration of Mexico and Canada into the US-led production system, reflecting the consolidation of the NAFTA trading bloc. A parallel and equally significant evolution is the shifting hierarchy within the Asian regional bloc. In the 1995-1999 period, Japan is the undisputed “key play hub” for Asia. However, by the 2010-2014 and 2020-2023 periods, China has clearly emerged as a primary hub in its own right, developing its own strong cluster of trade partners. This visual transformation is precisely reflected in quantitative metrics. The rising influence of China and South Korea, reflected in their high average betweenness scores, signals their new role as essential intermediaries in the GVC, aligning with the literature on their critical position in new EV and battery supply chains (Hu et al., 2021). These trends illustrate that while the original core hubs remain dominant, new powers and regional blocs are actively reshaping global trade flows.

3.2 Disaggregated topologies of automotive trade

The aggregate view of the automotive industry masks critical distinctions in the network structures of its constituent parts, a phenomenon observed by Gorgoni et al. (2018) . Our analysis confirms that the GVC is not monolithic; rather, it is a composite of at least three distinct network topologies corresponding to different stages of production. As visualized in Figure 3, comparing the network structures of 1995 against 2023 reveals a profound reorganization of the global industrial base, driven by divergent structural logics at each layer.

The most dramatic topological shift occurs in the feeder system for raw and semi-processed materials (bottom panel). In 1995, this network was defined by fragmented regionalism, organized into separate blocs: a European cluster dominated by Germany, and a distinct Asia-Pacific/Americas bloc anchored by the United States and Japan. By 2023, this multipolar structure collapsed into a centralized "uni-polar" system. China has emerged as the singular hub for global raw materials, visually replacing the fragmented networks of the past. The graph reveals that China now acts as the primary gravitational centre, connecting a diverse periphery of resource exporters directly into its industrial complex, effectively dissolving the regional silos that defined the 1990s.

In the network for parts and components, the evolution is characterized by intense densification and a shifting hierarchy in Asia. While the United States and Germany remain the persistent architects of the North American and European production fortresses, the overall network has become significantly denser, indicating the entry of numerous new players into the value chain. Most critically, the topology highlights a major geopolitical realignment in Asia: China has risen to become a key structural node, eclipsing Japan in terms of centrality and node size. This signals that the "Global Factory" is no longer just a story of Western dominance; it has evolved into a tri-polar system where China now functions as a primary industrial engine alongside the US and Germany, actively bridging regional supply chains.

Finally, the market interface for finished vehicles displays a remarkable stability in its fundamental shape, even as the cast of actors expands. Across both periods, the network retains a consistent "hub-and-spoke" distribution model, where Germany and Japan remain the dominant sources of export flow and the United States functions as the primary sink. However, the 2023 topology reveals the growing prominence of emerging economies: China, Mexico, and Canada have solidified their roles, transitioning from peripheral players to significant nodes within the global distribution system. Despite these new entrants, the overarching logic remains one of concentrated production feeding a diffuse global market, with the traditional industrial powers still holding the centre of the panel.

Figure 3: Automotive trade network at disaggregated dimension

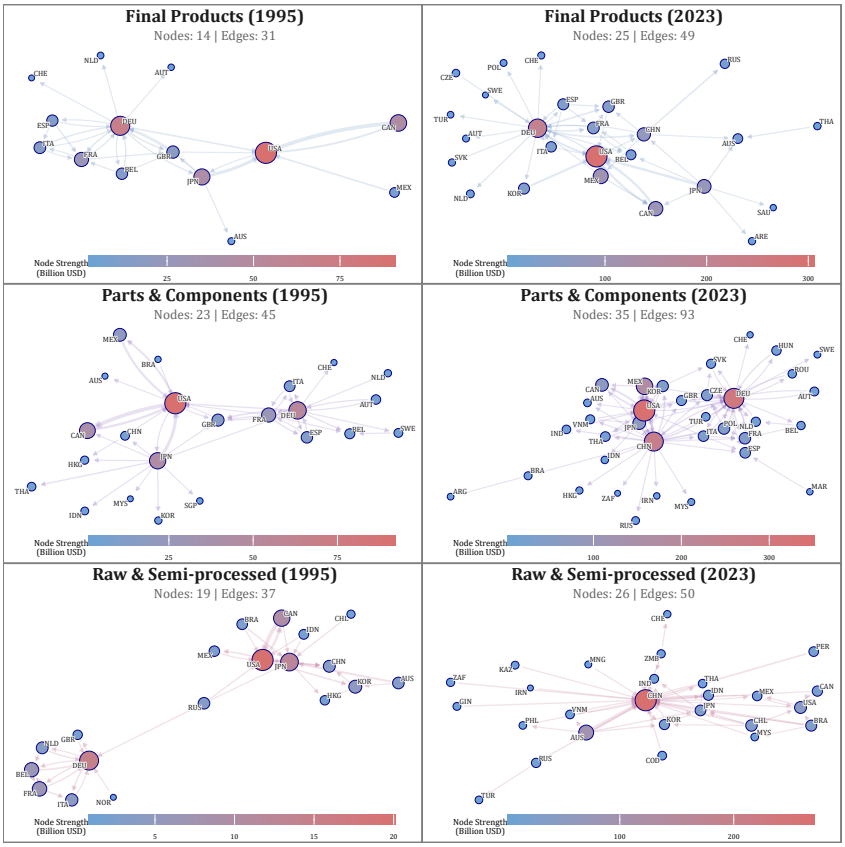

Note: The threshold was set at the top 0.5 percentile to suppress minor flows and highlight the structural backbone of the global trade network. Crucially, the filtering was applied independently within each time bin.

3.3. The emergent electric vehicle global value chain: A new structural paradigm

The emergence of the Electric Vehicle (EV) supply chain represents not a gradual evolution but a rapid and large-scale industrial reconfiguration. This transformation is visually evident in Figure 4 which tracks the topological evolution of the network from 2017 to 2023. In the initial period, the global EV network exhibited a loosely connected and multipolar structure characterized by distinct regional clusters anchored separately by Germany, the United States, and China. By 2023, this topology had shifted radically. The separated clusters have coalesced into a hyper-dense and globally integrated system. However, this integration has not resulted in a decentralized web. Rather, it has formed a monocentric system. The United States and major European economies have integrated more tightly than in the traditional automotive sector, yet China remains the dominant hub within the global EV network.

This network reconfiguration is accompanied by an inverted concentration hierarchy across the supply chain. Analysis of market share concentration (Figure 5) reveals

Figure 4: Network evolution of the electric vehicle trade (2017-2023)

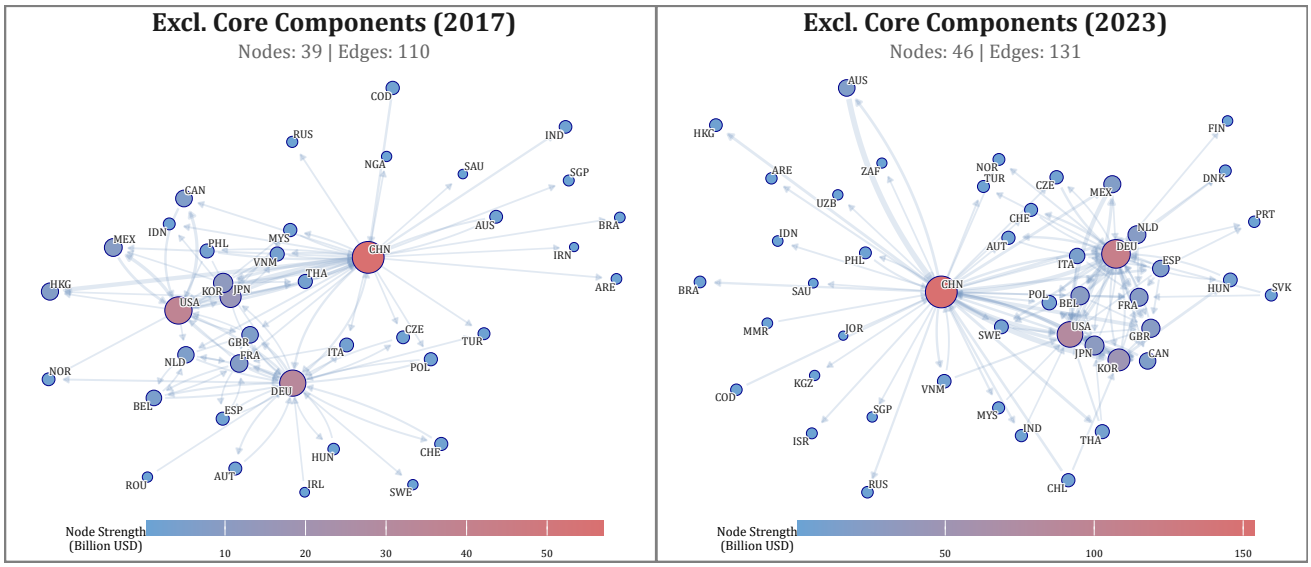

Note: The threshold was set at the top 1 percentile to suppress minor flows and highlight the structural backbone of the global trade network. Crucially, the filtering was applied independently.

Figure 5: Evolution of top (3) exporters' market share in automotive (HS92) and EV (HS17) supply chains

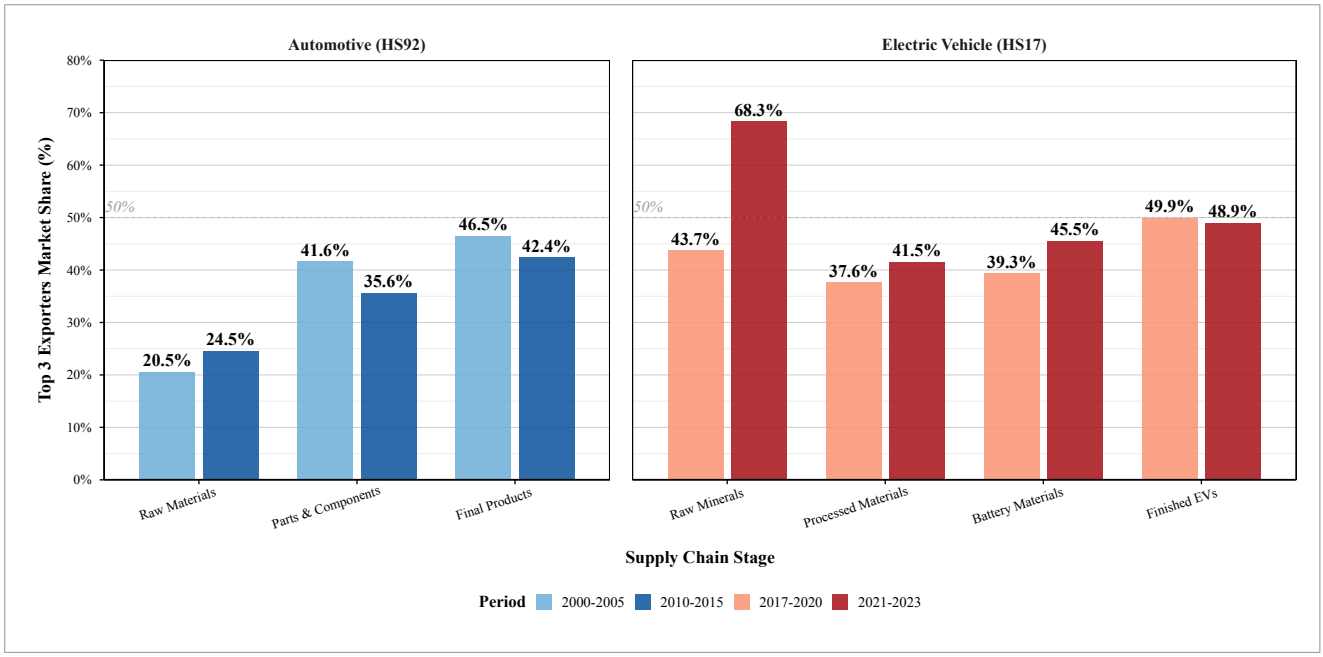

systematic variation across supply chain stages, with control tightening most intensely upstream rather than downstream. In the initial period (2017-2020), concentration was relatively balanced: raw materials (43.7%), processing (37.6%), and component manufacturing (39.3%) showed comparable levels among top three exporters. By the recent period (2021-2023), this equilibrium had dissolved. Raw material concentration surged to 68.3%, while processing rose more modestly to 41.5% and components to 45.5%. The 24.6 percentage increase in upstream concentration, vastly exceeding changes in processing and components, indicates that supply control has consolidated most dramatically at the extraction stage, inverting conventional expectations that concentration intensifies at points of greater technical complexity.

Raw material markets represent the most concentrated stage of the electric vehicle supply chain, with the top three exporters accounting for 68.3% of global trade in 2021–2023. Yet, as shown in

Figure 6, the network topology reflects import aggregation rather than export dominance. The upstream trade network is sparse (28 nodes, 44 edges), and China operates as the central hub, absorbing flows of lithium from Australia and Chile, cobalt from the Democratic Republic of Congo, and nickel from Indonesia and the Philippines. This hub-and-spoke structure channels geographically dispersed raw materials into China for processing and subsequent re-export as refined products. Chile stands out as an outward hub, shipping lithium carbonate directly to Germany, Japan, and South Korea, indicating that some midstream processors bypass Chinese intermediaries. The network's low edge density mirrors geological constraints: participation as an exporter requires economically viable deposits of battery-grade lithium (spodumene or brine), cobalt, nickel, or natural graphite. These resource limitations create structural concentration, and China's role as the dominant aggregation and processing point amplifies the concentration effects observed in market-share data.

The midstream network (Figure 6) comprises 35 nodes and 75 edges, indicating moderate density and broader geographic dispersion than the upstream stage. This structure resembles the "robust-yet-fragile" network described by Hu et al. (2021) , characterized by high efficiency but significant vulnerability to disruptions at key nodes. Within this structure, China occupies the network core, displaying the highest connectivity and intermediary positioning, while Germany, South Korea, Japan, and the United States appear as secondary hubs that establish multiple paths across midstream trade. In contrast, core component manufacturing is markedly more centralized: concentration rises to 45.5%, and the network assumes a star-like topology centred on China as the dominant outward hub, with 42 nodes and 151 edges and a high share of direct links from China to other participants. South Korea and Japan function as secondary nodes in this downstream configuration, but the edge pattern indicates that most connections radiate from the Chinese hub, consistent with the observed increase in centralization.

Finished vehicle trade exhibits unexpectedly high concentration (48.9% among top three exporters in 2021-2023), approaching levels observed in battery materials (45.5%) and exceeding processed materials (41.5%). The network topology (Figure 6) reveals a bipolar structure where Germany functions as the dominant hub, with the United States as a substantial secondary hub. The network displays sparse connectivity (22 nodes, 36 edges) relative to midstream components, yet concentration remains elevated due to Germany's commanding position in European exports and the United States' dominance in North American markets. Germany's hub centrality is visible in dense connections to European countries including Belgium, France, Spain, Italy, and Sweden, while the United States anchors a North American cluster linking Canada, Mexico, and Japan. China appears as a medium-sized node rather than peripheral, indicating significant export activity beyond domestic consumption, though its network position remains less central than Germany or the United States. This topology differs fundamentally from core components, where China's hub dominance is overwhelming, yet the concentration level (48.9%) suggests that final vehicle assembly, despite being geographically less constrained than mineral extraction, remains concentrated in established automotive manufacturing regions.

This analysis highlights the coexistence of two fundamentally different global value chains. The traditional automotive GVC, as documented by Russo et al. (2022), is a mature system characterized by regionalised co-production networks and concentration in final assembly and tier-1 suppliers, reflecting a gradual globalization process anchored by North America, Europe, and Japan. In contrast, the emerging EV value chain represents a new industrial paradigm with a markedly different architecture. Figures 4 through 6 reveal a structural funnel channelling resources from diffuse upstream raw mineral extraction (28 nodes, 44 edges, 68.3% concentration) through highly concentrated midstream processing and battery manufacturing (42 nodes, 151 edges in star topology, 45.5% concentration) before expanding into downstream vehicle assembly (22 nodes, 36 edges). This creates chokepoints that have become the focal point of the contemporary "race for critical minerals" (Kalantzakos, 2020). The locus of power resides not in downstream assembly but in control over intermediate goods within the midstream, where China has established a dominant structural position: functioning as inward hub aggregating raw materials from Australia, Chile, DRC and others, as processing centre converting minerals into battery-grade compounds, and as outward hub exporting battery cells to virtually all network participants.

These structural divergences carry significant strategic implications. For established automotive powers (EU, US, Japan), the analysis underscores a common vulnerability: industrial leadership in the traditional GVC does not automatically confer advantage in the EV paradigm. Germany and the United States dominate finished vehicle networks yet occupy peripheral positions in midstream battery components, where Chinese hub centrality is overwhelming. These economies exhibit pronounced dependency on an Asian-centric supply chain for critical midstream segments, particularly processed minerals and battery components. For emerging economies, the transition presents both opportunities and challenges. Resource-rich nations in Africa and Latin America have become indispensable upstream suppliers, visible in the sparse network topology, but face the imperative of moving beyond raw material extraction to capture greater value. Countries such as Germany in processed materials, South Korea, and Japan in battery cells demonstrate that the reconfiguration creates pathways for industrial upgrading, though they remain secondary to China's hub position. The overarching implication is that the EV transition has initiated a profound economic and geopolitical realignment. Mastery of the legacy automotive paradigm no longer guarantees leadership in the new system. The funnel structure creates vulnerability where concentration and centralization coincide upstream geological constraints (68.3%) limit diversification options, while midstream star topology indicates disruptions in Chinese production nodes would propagate rapidly given sparse alternative pathways. This results in a more complex, competitive, and strategically contested global landscape where power resides in controlling battery production rather than vehicle assembly.

Figure 6: Network evolution of the electric vehicle trade (2012-2023)

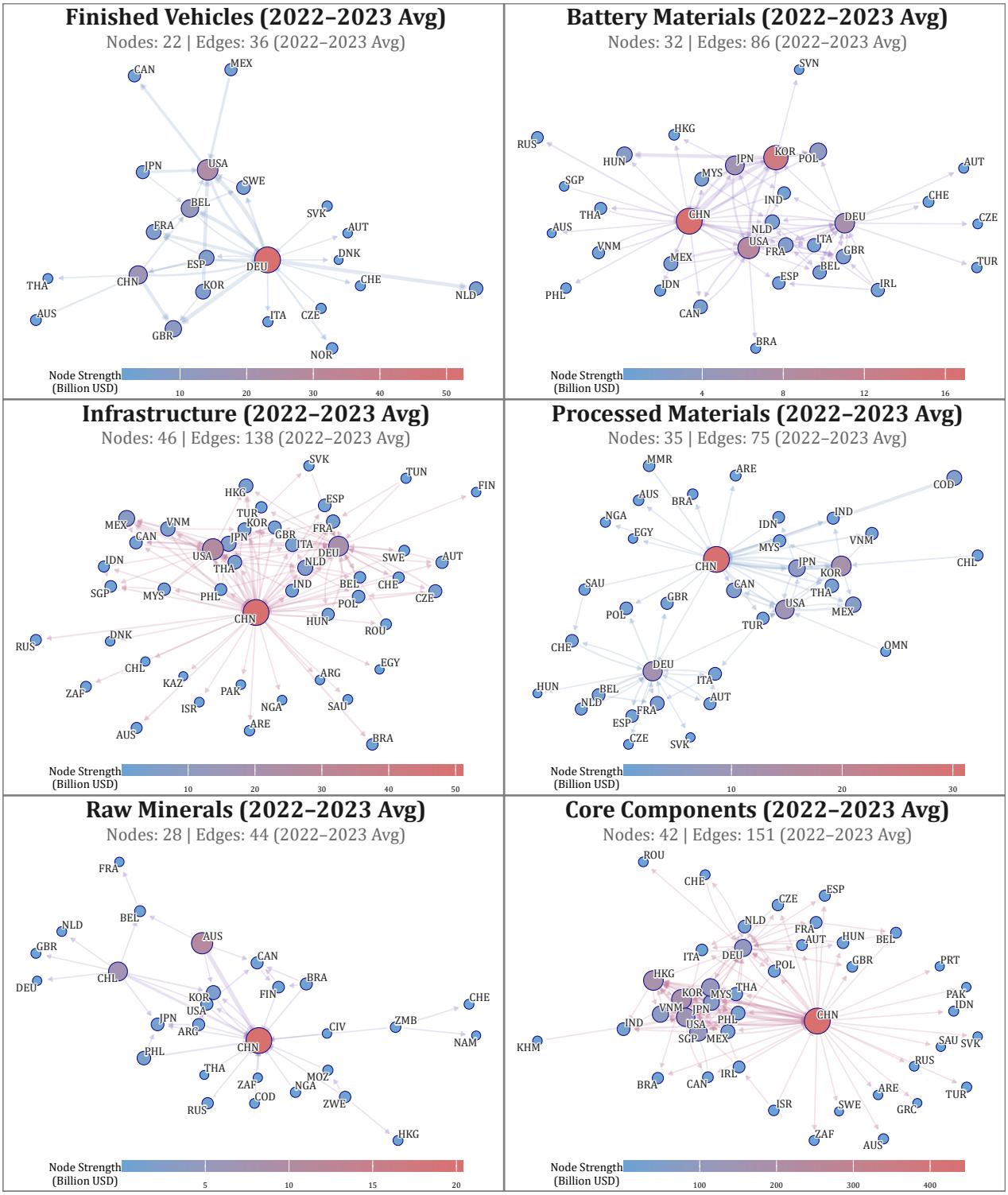

Note: The threshold was set at the top 1 percentile to suppress minor flows and highlight the structural backbone of the global trade network. Crucially, the filtering was applied independently.

4. Network modeling

4.1 Main estimation

Following the abstract graphing of the GVC's evolution, this section proceeds to an inferential analysis that statistically explains the drivers of network formation. To achieve this, we employ two complementary modelling approaches. The Temporal Exponential Random Graph Model (TERGM) is used to understand the forces shaping the structure of bilateral trade relationships in HS92 chapter 87 (vehicle and parts), capturing not only exogenous economic and geographic factors but also endogenous, self-organizing network dynamics. For comparison, a standard Poisson Pseudo Maximum Likelihood (PPML) gravity model is estimated to assess the determinants of trade volume, providing a complementary perspective on the intensity of these trade ties. This dual approach enables a more comprehensive understanding of both the formation and intensity of trade relationships, which is crucial for designing effective trade and industrial policies.

Table 1. TERGM estimation result

Variables	TERGM (1) HS92 Automotive	TERGM (2) HS92 Automotive	TERGM (3) HS Section 17
Network Structure			
Edges (Intercept)	-24.09	-14.84	-14.76
	[-24.92, -23.33]	[-15.53, -14.13]	[-15.50, -14.07]
Reciprocity (Mutual)	1.01	0.55	0.69
	[0.92, 1.10]	[0.48, 0.64]	[0.62, 0.75]
Triadic Closure (GWESP)	0.92	0.63	0.9
	[0.67, 1.16]	[0.46, 0.80]	[0.70, 1.08]
Dyadic Covariates (Gravity)			
Ln (Distance)	-0.89	-0.57	-0.54
	[-0.91, -0.87]	[-0.60, -0.54]	[-0.56, -0.51]
Contiguity	0.74	0.32	0.33
	[0.67, 0.79]	[0.24, 0.39]	[0.25, 0.40]
Policy Variables			
Trade Agreement	0.29	0.19	0.17
	[0.27, 0.31]	[0.16, 0.22]	[0.13, 0.20]
Ln (Applied Tariff + 1)	-0.1	-0.06	-0.05
	[-0.13, -0.07]	[-0.09, -0.04]	[-0.07, -0.03]
Nodal Covariates			
Ln (GDP Exporter) (Sender)	1.08	0.68	0.67
	[1.06, 1.11]	[0.66, 0.70]	[0.65, 0.69]
Ln (GDP Importer) (Receiver)	0.16	0.08	0.09
	[0.13, 0.19]	[0.05, 0.10]	[0.07, 0.11]
Ln (Population Exporter) (Sender)	-0.24	-0.15	-0.18
	[-0.28, -0.21]	[-0.17, -0.13]	[-0.21, -0.16]
Ln (Population Importer) (Receiver)	0.15	0.11	0.09
	[0.14, 0.16]	[0.10, 0.12]	[0.08, 0.11]
Temporal Terms			
Memory (Stability)		1.66	1.58
		[1.63, 1.70]	[1.55, 1.61]
Delayed Reciprocity		0.23	0.31
		[0.16, 0.28]	[0.25, 0.36]

Note: For each variable, the first row reports the bootstrap mean coefficient based on 1,000 resamples, rounded to two decimal places. The second row, in brackets, presents the 95% percentile confidence interval. Because p-values and standard errors may be unreliable when the bootstrap distribution deviates from normality, statistical significance is assessed by whether the confidence interval excludes zero. All models are specified as TERGMs, except Model (1), which is a static ERGM. The number of time steps is indicated for each specification (e.g., N = 29 for HS92 and N = 7 for HS17), with a one-period lag structure applied. To minimize noise and avoid periods with near-empty networks, the lowest 30% of trade values were excluded across all models. Full estimations and goodness-of-fit test results are reported in the supplementary tables, along with additional estimations for other product categories provided in the appendix.

To understand the complex evolution of global value chains (GVCs), we employ a Temporal Exponential Random Graph Model (TERGM). Unlike traditional gravity models that treat trade ties as independent observations, the TERGM is designed to analyse the network. Its unique contribution lies in its ability to simultaneously model the endogenous (network-native) properties of GVCs (such as their tendency to cluster and form reciprocal relationships) alongside exogenous (external) factors, including trade policy and geography. This approach allows us to untangle the effects of policy from the network's own self-organizing and path-dependent dynamics. The model estimates the probability of a trade tie forming or persisting, offering a powerful lens into how GVCs are structured and why they evolve over time.

The results, presented in Table 1, first highlight the endogenous structural properties of the trade network (using Model 2 as the reference). The large negative Edges coefficient (-14.84) establishes a baseline of network sparsity, confirming that significant international trade ties are relatively rare and their formation is a highly selective, non-random process. The model finds strong evidence for two key self-organizing principles. First, the positive and significant Reciprocity (Mutual) coefficient (0.55) validates the high levels of two-way, intra-industry trade. This indicates that when one trade partner exports to another, there is a significantly higher likelihood of a reciprocal trade relationship existing in the opposite direction. Second, the Triadic Closure (GWESP) coefficient is positive and significant (0.63), providing a statistical signature of supply chain formation. This finding of triadic closure (that a country's trading partners are likely to trade with each other) constitutes the micro-foundation of the dense, clustered production networks. For example, if a German parts supplier trades with an assembly plant in Mexico, and that plant also sources from a U.S. electronics firm, this transitive effect increases the likelihood of a direct trade relationship forming between the German and U.S. firms.

The temporal terms confirm that the network's evolution is highly path dependent. The significant Memory (Stability) term (1.66) is a powerful indicator of structural inertia, showing that existing trade ties are overwhelmingly likely to persist in the next step. This reflects the "stickiness" of GVCs, where high setup costs and established relationships create strong path dependence. Furthermore, the positive Delayed Reciprocity term (0.23) reveals a dynamic process of relationship-building, suggesting that one-way ties are likely to be reciprocated in future time steps, gradually deepening the network's integration.

Finally, the model assesses the impact of exogenous policy variables while controlling for these complex network dynamics. The Trade Agreement coefficient is positive and significant (e.g., 0.19 in Model 2), indicating that formal agreements successfully promote the formation of new trade ties. Conversely, the effect of tariffs emerges as a key inhibitor. The statistically significant and negative coefficient for Ln (Applied Tariff + 1) (-0.06) demonstrates that tariffs reduce the probability of forming new trade ties. This finding isolates the impact of tariffs on the extensive margin, implying they discourage the establishment of new supply chain relationships and constrain the expansion of GVCs. Taken together, these results show that GVCs evolve as stable, clustered, and path-dependent ecosystems, but their formation and expansion remain highly sensitive to trade policy interventions.

4.2 Value chain heterogeneity: Network structure meets policy sensitivity

While the aggregate analysis in Table 1 reveals fundamental network properties, these structural patterns vary systematically across value chain stages in ways that directly correspond to the topological features documented in Section 3. To test whether the concentration patterns and hub structures observed in our network mapping translate into measurable differences in trading behaviour, we re-estimate Model 3 separately for each supply chain segment. This approach enables us to assess whether upstream concentration and downstream clustering, identified through network topology, manifest as distinct endogenous network dynamics, such as reciprocity and triadic closure, as well as differential policy responsiveness to trade agreements and tariffs. Figure 7 presents log-odds coefficient estimates with 95% confidence intervals for the same core parameters from our main specification, now disaggregated by value chain stage. The results reveal three interconnected findings that bridge our descriptive network analysis with the inferential TERGM framework, highlighting the structural divergence between traditional automotive (HS92) and electric vehicles (HS17).

First, asymmetric reciprocity patterns validate hub-and-spoke topologies while revealing stark differences between automotive paradigms. Traditional automotive (HS92) exhibits relatively uniform reciprocity coefficients across raw materials (0.68), parts and components (0.67), and final products (0.46), reflecting mature, balanced supply relationships. The EV value chain (HS17) displays pronounced asymmetry. Battery materials exhibit substantially weaker reciprocity (0.36), confirming unidirectional flows from resource exporters, such as Chile and the DRC, to processing hubs, with minimal reverse flows. Most strikingly, EV finished vehicles exhibit the lowest reciprocity coefficient (0.19), which is significantly lower than that of traditional automotive final products and even lower than that of battery materials. This indicates that, conditional on the rest of the network, EV final assembly involves highly asymmetric trade patterns concentrated among established automotive powers (Germany, the US, and China) who export to consuming markets but do not engage in balanced two-way trade. This extends Gorgoni et al. (2018) by demonstrating that the endogenous network formation process generates hierarchical asymmetry that intensifies at both ends of the EV value chain, where geological constraints (upstream) and manufacturing concentration (downstream) are most binding.

Second, triadic closure patterns mirror the concentration funnel while revealing how the EV transition reshapes clustering dynamics. Traditional automotive shows moderate and relatively uniform closure coefficients across raw materials (0.62), parts and components (0.88), and final products (0.46), indicating established regional production networks. The EV value chain displays extreme variation. Battery materials exhibit the weakest closure (0.22), confirming that hub intermediaries, such as China, do not create peripheral triangles between suppliers and consumers. Notably,

Figure 7: TERGM estimates for automotive and electric vehicle trade networks across value chain stages

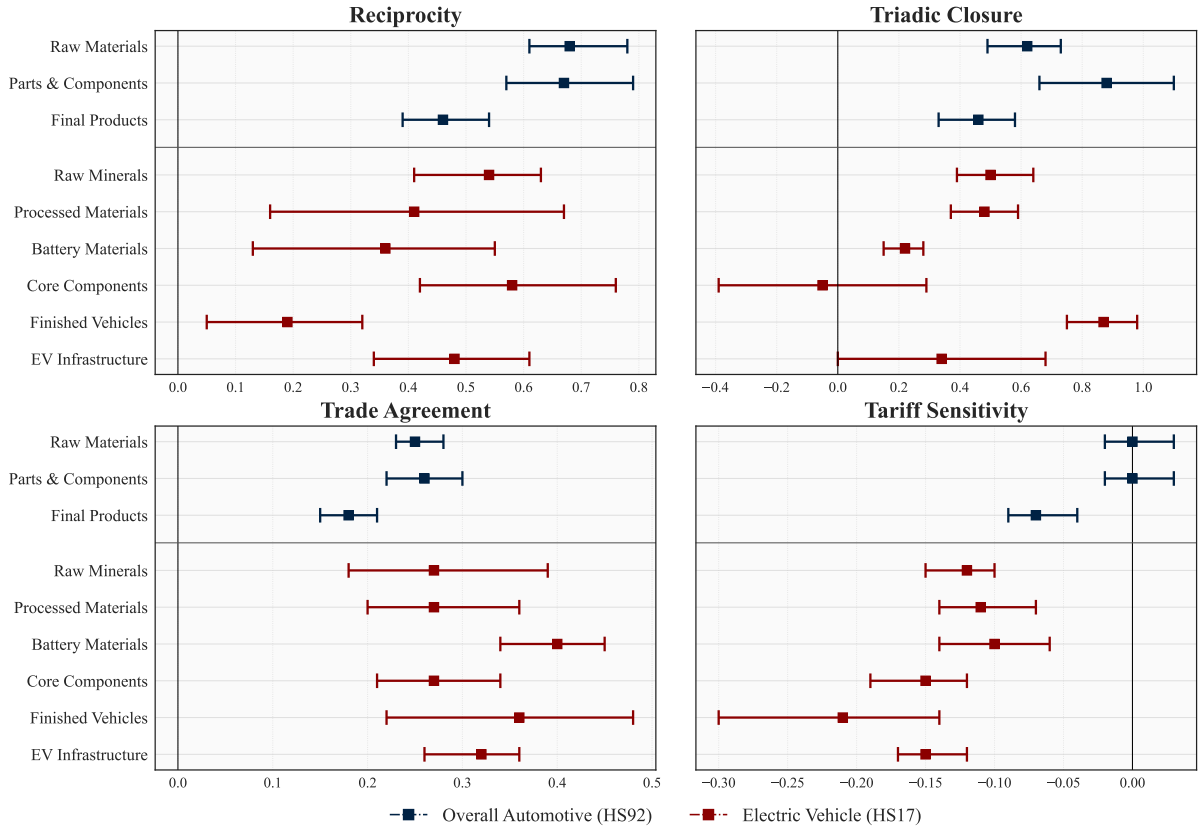

Note: Specification identical to TERGM (Model 3), applied to distinct trade-flow outcomes by value-chain stage; see appendix for full estimates.

EV core components exhibit negative triadic closure (-0.05), suggesting that, conditional on other network structures, trading partners tend toward anti-clustering rather than triangle formation. This likely reflects strategic competition and supply chain segmentation in the battery cell and electric motor industries, where firms establish exclusive bilateral relationships rather than integrated regional networks. In sharp contrast, EV finished vehicles display the strongest closure (0.87), significantly exceeding traditional automotive final products, indicating that final assembly remains concentrated in tightly clustered regional production systems. This progression from negative closure in core components (-0.05) to high closure in finished vehicles (0.87) provides micro-foundations for the "robust-yet-fragile" structure cited from Hu et al. (2021). Downstream clustering creates redundant pathways, yet upstream hub-and-spoke structures (0.22 for battery materials) and midstream anti-clustering (-0.05 for core components) result in disruptions propagating rapidly through sparse, non-overlapping supply chains.

Third, policy sensitivity patterns in Figure 6 reveal stark contrasts between EV and traditional automotive value chains, with critical implications for border adjustment mechanisms. Traditional automotive shows moderate, uniform trade agreement effects across stages (0.18-0.26) and negligible tariff sensitivity, reflecting mature supply chains that have been adapted through preferential regimes. The EV chain displays markedly different dynamics. Battery materials exhibit the strongest trade agreement effect (0.40, significantly exceeding traditional automotive) combined with weak triadic closure (0.22), suggesting bilateral agreements can catalyse diversification in sparse upstream networks. However, EV stages exhibit substantial tariff sensitivity, with finished vehicles being the most vulnerable (-0.21), followed by core components and infrastructure (-0.15), and battery materials (-0.10). This asymmetric policy responsiveness reveals that while trade-facilitating agreements promote network formation, price-based barriers disproportionately disrupt EV supply chains compared to traditional automotive. The elevated sensitivity to both instruments suggests emerging EV networks remain highly malleable to trade policy interventions, whether market-opening agreements or border-adjustment mechanisms, contrasting sharply with the policy-adapted resilience of traditional automotive supply chains.

The stage-specific dynamics revealed in Figure 6 demonstrate that the EV supply chain represents a fundamental restructuring rather than an extension of automotive trade networks. Traditional automotive exhibits moderate reciprocity, uniform triadic closure, and minimal policy

sensitivity across all stages, reflecting mature, resilient regional co-production systems. In sharp contrast, the EV chain exhibits extreme structural variation: geological constraints result in low reciprocity upstream (0.36), competitive dynamics lead to anti-clustering in midstream (-0.05), and manufacturing concentration yields low reciprocity but high clustering downstream (0.19 vs. 0.87). Most critically, this structural divergence translates into asymmetric policy exposure. The high trade agreement leverage in battery materials (0.40) combined with sparse networks (0.22 closure) suggests upstream diversification strategies can gain traction through bilateral agreements. However, the elevated tariff sensitivity throughout EV stages (-0.10 to -0.21) reveals a fundamental vulnerability: unlike traditional automotive, which has adapted to existing trade barriers, the emerging EV network remains highly susceptible to border adjustment mechanisms precisely now when integration is needed for scale economies and learning effects. This policy malleability creates both opportunity and risk for the transition.

Synthesis of TERGM and gravity PPML findings

To further contextualize our TERGM findings, we estimated a series of PPML gravity models to examine the intensive margin (trade volume), with results in Table 2. Our most robust specifications, Models 3 and 6, employ directional fixed effects (specifically, exporter-year and importer-year fixed effects). This advanced specification is critical as it non-parametrically controls for all time-varying, country-specific unobserved factors and effectively accounts for multilateral resistance. A consistent finding emerges when these powerful fixed effects are included to produce robust results: the coefficients for both trade agreements and tariffs are significantly attenuated. This highlights the complementary nature of our two methods. The TERGM is designed to capture endogenous network dependencies, while the PPML with directional fixed effects excels at isolating effects from unobserved heterogeneity and the multilateral resistance term. The divergence in results is therefore not a contradiction, but a crucial finding that helps specify the precise channel through which policy influence operates.

This interpretation is supported by the coefficients in Table 2. In Model 3 (HS92 Automotive), the Trade Agreement (0.143) and Tariff (-0.083) coefficients, while still statistically significant, are substantially smaller than in baseline models. This pattern is amplified in Model 6 (HS17 EV), where both the Trade Agreement (0.049) and Tariff (-0.253) coefficients are not statistically significant. We propose that these PPML findings are complementary and serve to validate our TERGM-based conclusions. Policy appears to function as a critical facilitator of, or barrier to, market entry. This is an effect on the extensive margin that the TERGM, with its focus on network structure, was uniquely suited to capture. Once a trade relationship is established, however, its subsequent volume (the intensive margin) appears to be driven far more by the powerful, time-varying economic fundamentals that the PPML's directional fixed effects successfully isolate. A study relying solely on one method would miss part of the story; our TERGM correctly identified the structural role of policy, while our robust PPML analysis confirms that this effect is distinct from the drivers of the intensive margin.

Table 2. Gravity model estimation result

Variable	PPML (1)	PPML (02)	PPML (3)	PPML (4)	PPML (5)	PPML (6)
	HS92 Automotive Trade (1995 - 23)			HS17 EV Trade (2017-2023)		
Dyadic Covariates (Gravity)						
Ln (Distance)	-0.327***	-0.404***	-	-0.508***	-0.263***	-
	(-18.82)	(-22.42)		(-13.96)	(-10.02)	
Contiguity	1.152***	0.864***	0.662	0.345***	0.830***	-
	-25.87	-29.19	-1.22	-3.62	-12.17	
Policy Variables						
Trade Agreement	0.830***	0.653***	0.143**	1.029***	0.483***	0.049
	-23.85	-24.22	-2.58	-8.53	-6.08	-0.62
Ln(Applied Tariff)	-0.262***	-0.586***	-0.083**	-0.047	-0.230***	-0.253
	(-13.46)	(-31.45)	(-2.83)	(-0.94)	(-5.96)	(-1.75)
Nodal Covariates						
Ln (GDP Exporter)	1.086***	0.892***	-	0.845***	0.835*	-
	-72.08	-23.25		-35.56	-2.55	
Ln (GDP Importer)	0.847***	0.645***	-	0.912***	0.216	-
	-43.78	-15.17		-29.79	-0.68	
Ln (Pop-Exporter)	-0.173***	-0.39	-	0.140***	-3.132	-
	(-11.41)	(-1.75)		-4.27	(-1.68)	
Ln (Pop-Importer)	-0.012	-0.396***	-	-0.105**	1.837	-
	(-0.77)	(-4.50)		(-2.82)	-1.36	
Constant	-34.94***	-11.54**	14.75***	-33.38***	11.93	15.39***
	(-74.89)	(-2.86)	-82.72	(-38.41)	-0.26	-98.99
N Observations	1,003,255	1,003,255	746,304	242,165	242,165	138,810
Pseudo R^2	0.825	0.929	0.991	0.714	0.919	0.992
Fixed Effects						
ID (Direct Pair) FE	No	Yes	No	No	Yes	No
Exporter-Year FE	No	No	Yes	No	No	Yes
Importer-Year FE	No	No	Yes	No	No	Yes
Year + Partner FEs	No	Yes	No	No	Yes	No

Note: The coefficients presented are derived from Poisson Pseudo-Maximum Likelihood (PPML) gravity regressions, which were estimated using the ppmlhdfe command, with robust t-statistics reported in parentheses. Standard errors for columns (3) and (6) are clustered at the country-pair (dyadic) level. Significance is denoted by * p<0.05, **p<0.01, and *** p<0.001. Due to perfect collinearity with the comprehensive set of fixed effects, both time-invariant dyadic variables (e.g., distance) and country-year specific variables (e.g., GDP, Population) are omitted. An exception is the Contiguity dummy in the HS92 specification, which retained its coefficient, as it varies over time due to specific geopolitical events, such as a state division or change in internationally recognized borders, which affects the calculation of contiguity for neighboring economies in that period. The significant drop in observations should be noted, as this is a consequence of the fixed-effects procedure dropping singletons or groups separated by the fixed effects; the Contiguity variable was also likely omitted from the HS17 EV specifications. The dependent variables are bilateral trade flows (in thousands USD) for the indicated HS92 or HS17 product aggregations, with full model details provided in the Appendix.

5. Discussion, policy implications, limitations, and future research

This paper presents a multi-stage empirical analysis of the structural transformation of the global automotive industry during the electric vehicle (EV) transition. The findings suggest that the EV transition is associated with a noticeable reorganisation of automotive trade networks, but within a broader structure that remains highly path-dependent. At the aggregate level, traditional automotive trade continues to display the well-documented features of a mature GVC: regional production blocs centred on Europe, North America, and East Asia; moderate reciprocity; and relatively uniform triadic closure. By contrast, the EV-related networks in our sample are more concentrated upstream and in parts of the midstream and exhibit a "funnel-like" configuration with relatively sparse raw-material trade, more centralised processing and core components, and a somewhat more dispersed pattern for finished vehicles. The TERGM estimates indicate that, for both traditional and EV-related products, network evolution is characterized by strong temporal dependence and endogenous structuring: existing ties are highly persistent, and the likelihood of new ties is associated with reciprocity, shared partners, and standard gravity covariates, such as distance and contiguity. Within this general pattern, policy instruments exert a distinct influence across the different dimensions of trade. Trade agreements facilitate the extensive margin by increasing the likelihood of tie formation, whereas higher tariffs act as a dual constraint: they significantly reduce the probability of creating new linkages and, as confirmed by our complementary PPML estimates, suppress the intensive margin of existing trade volumes.

Within this global context, the results indicate a specific configuration of exposure for the European Union (EU). In the EV-related networks identified, while Germany remains a key outward hub in finished-vehicle exports, its position in midstream EV segments is predominantly inward-facing, with trade concentrated through a narrow set of major hubs led by China. This aligns with external evidence that the EU is significantly import-dependent for several critical raw materials and many processed battery inputs, and that a substantial portion of the cell manufacturing capacity serving the European market is based in East Asia. At the same time, the degree of dependence varies across specific materials and over time, and the network measures used here cannot distinguish between different forms of industrial and technological control. These patterns should therefore be interpreted as indicative of potential vulnerability in selected segments, not as a comprehensive assessment of EU dependence across the entire EV supply chain.

The TERGM results suggest that diversification strategies are likely to face frictions arising from network structure. Strong memory terms imply that once established, supply relationships tend to persist; reciprocity and triadic closure imply that new ties are more likely to form along existing pathways. In the case of battery materials, we observe weak but positive triadic closure alongside relatively strong positive associations between trade agreements and tie formation. Taken together, these findings are consistent with the idea that bilateral or regional agreements can facilitate entry by additional suppliers, particularly where there is already some prior economic or geographic linkage. However, they do not imply that such policies can easily reorient supply chains away from dominant hubs in the short term.

Regarding tariffs, our estimates suggest that EV-related flows during the studied period are, on average, more negatively associated with tariff increases than those for conventional automotive products, both in terms of tie formation probabilities and, in some specifications, trade volumes. This is broadly in line with other work showing that tariffs on EVs and parts can have non-trivial effects on trade and welfare. However, those studies also emphasize that impacts depend on where in the value chain tariffs are applied and how other policies respond. In light of these nuances, it is more accurate to say that EV-related flows in our sample appear relatively sensitive to tariff-like instruments, rather than to claim that such sensitivity is universal or invariant across contexts.

These observations have implications for how instruments such as the Critical Raw Materials Act (CRMA) and the Carbon Border Adjustment Mechanism (CBAM) might interact with existing network structures. CRMA aims at supplier diversification and risk reduction in critical raw materials; our results are consistent with the view that such aims are challenging, but not impossible, in a setting where existing hubs already intermediate many flows. CBAM, in its current form, applies to a defined set of carbon-intensive sectors (iron and steel, cement, aluminium, fertilisers, electricity, hydrogen, and some precursors and downstream products), and does not directly cover finished EVs, batteries, or most EV components. Any current impact on EV value chains is therefore indirect, operating through input costs rather than through direct pricing of batteries or vehicles. Discussions on extending carbon-based border measures to additional products are ongoing; our findings simply suggest that, if such measures were to be extended to EV-relevant products in the future, they could interact with supply chain formation in ways that warrant careful consideration.

Finally, although much of the analysis in this paper has emphasised the efficiency properties of dense, liberalised networks, there are also legitimate security concerns about high concentration at key nodes. Recent experience with export controls and sanctions has highlighted how central positions in global financial and production networks can be used for coercive purposes, a phenomenon that

Farrell and Newman (2019) describe as "weaponised interdependence". Our EV network results show midstream stages with hubandspoke structures that, in principle, could function as chokepoints. The present analysis does not attempt to assess the likelihood of deliberate supply denial, but it does indicate that, if such behaviour were to occur, its effects could be amplified by existing concentration. This reinforces the case for a cautious approach that weighs both efficiency and security considerations, without assuming that either objective can be fully maximized.

These conclusions are subject to several limitations. The analysis is based on gross trade flows rather than value-added measures, which may overstate the apparent centrality of economies that function as re-export hubs. The EV-specific time series is relatively short, reflecting the recent emergence of dedicated product codes, which constrains the precision of dynamic estimates. The treatment of trade agreements and tariffs is necessarily stylised, and non-tariff barriers and firm-level governance structures are not explicitly modelled. The empirical framework also remains within a partial equilibrium perspective, not incorporating feedback across sectors or factor markets.

These limitations point directly to an agenda for future research. Extending the analysis with trade in value-added data and firm-level ownership information would allow a clearer distinction between territorial and corporate control over EV supply chains. Incorporating environmental and social indicators would enable the assessment of whether the emerging configuration of EV GVCs aligns with broader sustainability objectives, rather than just decarbonisation targets narrowly defined. Finally, embedding the network structure identified here within a general equilibrium or simulation framework would permit systematic exploration of how different combinations of trade and industrial policies, including CBAM design choices, affect both the resilience and efficiency of the EV transition.

Acknowledgement: This research was funded by the Centre of Excellence for Trade and Environment, with support from the European Union and the European Education and Culture Executive Agency (EACEA).

References

BÖNING, J., DI NINO, V. & FOLGER, T. 2023. Benefits and Costs of the ETS in the EU, a Lesson Learned for the CBAM Design.

CAO, T. & HU, Y. 2025. Can Trade Policy Uncertainty Drive Green Innovation? Empirical Evidence From the US–China Trade War. *Australian Economic Papers.*

CIURIAK, D. 2025. Electric Vehicles: The Economics, the Geopolitics, and the Policy Lemmas Facing Europe. *Available at SSRN 5327778.*

CONTE, M., COTTERLAZ, P. & MAYER, T. 2022. *The CEPII gravity database,* CEPII Paris.

CSARDI, G. & NEPUSZ, T. 2006. The igraph software. *Complex syst,* 1695, 1-9.

DE BENEDICTIS, L., NENCI, S., SANTONI, G., TAJOLI, L. & VICARELLI, C. 2014. Network analysis of world trade using the BACI-CEPII dataset. *Global Economy Journal,* 14, 287-343.

DING, S., WANG, L. & ZHOU, Q. 2025. Study on Evolution Mechanism of Agricultural Trade Network of RCEP Countries—Complex System Analysis Based on the TERGM Model. *Systems,* 13, 593.

DOLPHIN, G. & FERRUCCI, G. 2025. The EU's CBAM: Implications for Member States and Trading Partners. International Monetary Fund.

ERDOGDU, E. 2025. The carbon border adjustment mechanism: Opportunities and challenges for non-EU countries. *Wiley Interdisciplinary Reviews: Energy and Environment,* 14, e70000.

FARRELL, H. & NEWMAN, A. L. 2019. Weaponized interdependence: How global economic networks shape state coercion. *International security,* 44, 42-79.

FENG, L., CHEN, B., WU, G. & ZHANG, Q. 2024. Global renewable energy trade network: patterns and determinants. *Environmental Science and Pollution Research,* 31, 15538-15558.

FRUCHTERMAN, T. M. & REINGOLD, E. M. 1991. Graph drawing by force-directed placement. *Software: Practice and experience,* 21, 1129-1164.

GAULIER, G. & ZIGNAGO, S. 2008. BACI: A World Database of International Trade at the Product-level (The 1995-2004 Version).

GORGONI, S., AMIGHINI, A. & SMITH, M. 2018. Automotive international trade networks: A comparative analysis over the last two decades. *Network Science,* 6, 571-606.

GUREVICH, T. 2018. The dynamic gravity dataset: 1948–2016. *USITC Working Paper, 2018–02–A.*

HANNEKE, S., FU, W. & XING, E. P. 2010. Discrete temporal models of social networks.

HU, X., WANG, C., ZHU, X., YAO, C. & GHADIMI, P. 2021. Trade structure and risk transmission in the international automotive Li-ion batteries trade. *Resources, Conservation and Recycling,* 170, 105591.

KALANTZAKOS, S. 2020. The race for critical minerals in an era of geopolitical realignments. *The International Spectator,* 55, 1-16.

LARCH, M. 2020. Mario Larch's Regional Trade Agreements Database from Egger and Larch (2008). *Retrieved November,* 29, 2020.

LARCH, M. & YOTOV, Y. V. 2024. Estimating the effects of trade agreements: Lessons from 60 years of methods and data. *The World Economy,* 47, 1771-1799.

LEIFELD, P., CRANMER, S. J. & DESMARAIS, B. A. 2018. Temporal exponential random graph models with btergm: Estimation and bootstrap confidence intervals. *Journal of Statistical Software,* 83, 1-36.

MAHUTGA, M. C. 2006. The persistence of structural inequality? A network analysis of international trade, 1965–2000. *Social Forces,* 84, 1863-1889.

PAN, X. & LIU, S. 2024. The development, changes and responses of the European Union carbon border adjustment mechanism in the context of global energy transition. *World Development Sustainability,* 4, 100148.

RUSSO, M., ALBONI, F., CARRETO SANGINÉS, J., DE DOMENICO, M., MANGIONI, G., RIGHI, S. & SIMONAZZI, A. 2022. The changing shape of the world automobile industry: A multilayer network analysis of international trade in components and parts.

SANON, S. & SLANY, A. 2023. Identifying African countries' potential in the African automotive industry – A continental supply chain mapping approach [Background paper commissioned for the 2023 Economic Development in Africa Report]. United Nations Conference on Trade and Development.

SILVA, J. S. & TENREYRO, S. 2006. The log of gravity. *The Review of Economics and statistics,* 641-658.

STURGEON, T., VAN BIESEBROECK, J. & GEREFFI, G. 2008. Value chains, networks and clusters: reframing the global automotive industry. *Journal of economic geography,* 8, 297-321.

TETI, F. 2024. Missing tariffs.

UNCTAD 2023. Supply chains, trade flows and value addition: Technical note on critical minerals (UNCTAD/DITC/MISC/2023/14). United Nations.

WASSERMAN, S. 1994. Social network analysis: Methods and applications. *The Press Syndicate of the University of Cambridge.*

YANG, S., KELLER, F. B. & ZHENG, L. 2016. *Social network analysis: Methods and examples,* Sage Publications.

YU, G., XIONG, C., XIAO, J., HE, D. & PENG, G. 2022. Evolutionary analysis of the global rare earth trade networks. *Applied Mathematics and Computation,* 430, 127249.

Appendix 01:

Classification of electric vehicle trade goods based on HS2017 (6-Digit Codes) – 17 codes

1. Battery materials (chemicals)

284190: Electrical Machinery and Equipment (8501) | 284290: Inorganic acid salts: silicates excluded, aluminosilicates included. | 382499: Chemical products, mixtures, and preparations: heading 3824. | 854590: Electrical carbon and graphite articles.

2. Core components and electronics

850110: Electric motors: output not exceeding 37.5W. | 850120: Universal AC/DC motors, over 37.5W output. | 850131: DC electric motors and generators under 750W. | 850132: DC motors/generators: 750W-75kW output. | 850133: DC motors/generators: 75kW < output ≤ 375kW | 850134: High-output DC electric motors and generators. | 850140: Single-phase AC electric motors. | 850151: AC multi-phase motors, up to 750W. | 850152: AC multi-phase motors, 750W-75kW output. | 850153: Multi-phase AC motors over 75kW. | 850161: AC generators, alternators, up to 75kVA. | 850162: AC generators: 75kVA-375kVA output. | 850163: AC generators: 375-750kVA output. | 850164: AC generators over 750kVA output. | 850300: Parts for electric motors and generators. | 850440: Static electrical power conversion devices | 850511: Permanent metal magnets and pre-magnetization articles. | 850760: Lithium-ion electric accumulators, including separators. | 850790: Parts of electric accumulators, not elsewhere specified. | 854110: Electrical apparatus: non-photosensitive, non-LED diodes. | 854121: Low-power non-photosensitive transistor electrical apparatus. | 854129: Transistors (non-photosensitive) dissipate 1W or more. | 854130: Electrical apparatus: thyristors, diacs, triacs (non-photosensitive) | 854140: Photosensitive electrical apparatus, including LEDs and PV cells. | 854150: Photosensitive semiconductor devices, including photovoltaic cells. | 854160: Mounted piezoelectric crystals. | 854190: Parts for semiconductor devices and apparatus. | 854231: Integrated circuits: processors, controllers, and associated circuits. | 854232: Memory: electronic integrated circuits for data storage. | 854233: Integrated circuit amplifiers: advanced electronic components. | 854239: Integrated circuits not elsewhere specified in HS8542. | 854290: Electronic integrated circuit components.

3. Finished vehicles

870240: Electric public transport vehicles: new or used. | 870360: Plug-in hybrid electric vehicles (PHEV) | 870370: Plug-in hybrid diesel vehicles for propulsion. | 870380: Electric vehicles: propulsion exclusively by electric motor.

4. Infrastructure

850440: Electrical static converter systems. | K63854442: Connectored insulated electric conductors, under 1000V.

5. Processed materials

280530: Rare earth metals: scandium and yttrium. | 282200: Commercial cobalt oxides and hydroxides. | 282520: Lithium compounds: oxides and hydroxides. | 284690: Inorganic/organic compounds of rare-earth, yttrium, scandium metals. | 380110: Artificial graphite. | 720915: Cold-rolled, flat, non-alloy steel, 3mm+ thick. | 720916: Cold-rolled non-alloy steel coils, 1-3mm thick. | 720917: Cold-rolled, flat, non-alloy steel, 0.5-1mm thick. | 720918: Cold-rolled non-alloy steel, less than 0.5mm thick. | 720925: Cold-rolled, flat iron/steel, ≥600mm width, ≥3mm thick. | 720926: Cold-rolled non-alloy steel, 1-3mm thick. | 720927: Cold-rolled flat iron/steel, 0.5-1mm thick. | 720928: Cold-rolled, flat, non-alloy steel, under 0.5mm. | 720990: Cold-rolled flat iron/steel, ≥600mm width. | 741011: Refined copper foil, thin and unbacked. | 741012: Thin, unbacked copper alloy foil. | 741021: Refined copper foil, <=0.15mm, with backing. | 741022: Copper alloy foil, backed, ≤0.15mm thick. | 760611: Rectangular aluminium plates, sheets, and strips. | 760612: Aluminium plates, sheets, strips, exceeding 0.2mm, alloys. | 760691: Non-alloyed aluminium plates, sheets, strips. | 760692: Non-rectangular/square aluminium alloy plates, sheets, strips. | 760711: Thin, unbacked, rolled aluminium foil (≤0.2mm). | 760719: Thin, unrolled aluminium foil, 0.2mm maximum. | 760720: Aluminium foil, backed, ≤0.2mm thick. | 810520: Cobalt: metallurgy intermediates, unwrought, and powdered forms.

6. Raw minerals

250410: Natural graphite, powdered or flaked. | 253090: Miscellaneous mineral substances, not elsewhere specified. | 260400: Nickel ores and concentrates are refined. | 260500: Concentrated cobalt ores and related materials. | 283691: Lithium carbonate within the carbonate family.

Appendix 02:

Classification of automotive goods based on HS1992 (6-Digit Codes) – 264 codes

1. Final products

870110: Pedestrian-controlled agricultural tractors | 870120: Road tractors for semi-trailers. | 870130: Track-laying tractors. | 870190: Tractors: heading 8701, excluding 8709. | 870210: Public transport vehicles: diesel, 10+ passengers. | 870290: Public transport vehicles, excluding diesel engine types. | 870310: Specialized vehicles for snow travel, golf, and similar uses. | 870321: Spark-ignition internal combustion engine vehicles under 1000cc. | 870322: Spark-ignition vehicles, 1000-1500cc engine capacity. | 870323: Spark-ignition internal combustion engine vehicles (1500-3000cc). | 870324: Spark-ignition engine vehicles over 3000cc. | 870331: Diesel vehicles: 1500cc cylinder capacity or less. | 870332: Diesel vehicles: 1500-2500cc compression-ignition engines. | 870333: Diesel/semi-diesel vehicles, engine capacity exceeding 2500cc. | 870390: Vehicles: personal transport, excluding certain classifications. | 870410: Off-highway dumpers for goods transport. | 870421: Diesel vehicles for goods transport (under 5T GVW). | 870422: Diesel goods vehicles, 5-20 tonnes gross weight. | 870423: Diesel goods vehicles, exceeding 20 tonnes GVW. | 870431: Spark-ignition vehicles: goods transport, under 5 tonnes. | 870432: Spark-ignition vehicles: goods transport exceeding 5 tonnes. | 870490: Goods transport vehicles, excluding heading 8704. | 870510: Heavy lifting vehicle: crane lorries. | 870520: Mobile drilling derricks for vehicular applications. | 870530: Firefighting apparatus. | 870540: Concrete-mixer lorries: vehicular assets. | 870590: Specialized vehicles: breakdown, road-sweeping, spraying, mobile workshops, radiological. | 871110: Auxiliary-motor cycles under 50cc, with or without side-cars. | 871120: Motorcycles: 50-250cc engine, with or without side-cars. | 871130: Motorcycles with side-cars, 250-500cc engine capacity. | 871140: Sidecars for motorcycles: 500-800cc engine capacity. | 871150: Side-cars for motorcycles over 800cc engines. | 871190: Motorcycles and cycles: side-cars with auxiliary motors. | 871640: Other trailers and semi-trailers.

2. Parts and components

392630: Plastic fittings for furniture and coachwork. | 392690: Miscellaneous plastic articles not elsewhere specified. | 400950: Vulcanised rubber tubes, pipes, and hoses with fittings. | 401110: Pneumatic rubber tires for motor vehicles. | 401120: New pneumatic rubber tires for buses or lorries. | 401140: Motorcycle new pneumatic rubber tire. | 401210: Retreaded rubber tires. | 401310: Motor vehicle inner tube rubber. | 401390: Rubber inner tubes, not elsewhere specified. | 401693: Vulcanized rubber gaskets, washers, and other seals. | 401699: Vulcanized non-cellular rubber articles, excluding hard rubber. | 481200: Paper pulp: filter blocks, slabs, and plates. | 681310: Asbestos and cellulose-based brake linings and pads. | 681390: Unmounted friction material: asbestos, mineral, or cellulose-based. | 700711: Vehicle/aircraft safety glass: toughened, shaped | 700721: Laminated safety glass for vehicles and spacecraft. | 700910: Automotive rear-view mirror glass. | 731511: Articulated roller chain, iron or steel. | 731811: Threaded iron or steel coach screws. | 731812: Threaded iron or steel wood screws. | 731813: Threaded iron or steel screw hooks and rings. | 731814: Threaded self-tapping screws, iron/steel. | 731815: Threaded iron or steel fasteners, with or without washers. | 731816: Threaded iron/steel nuts. | 731819: Threaded iron/steel fasteners, e.g., screws, bolts, and nuts. | 731821: Iron/steel non-threaded spring and lock washers. | 731822: Non-threaded iron/steel washers, excluding spring/lock types. | 731823: Non-threaded iron/steel rivets. | 731824: Non-threaded iron or steel cotters and cotter-pins. | 731829: Iron/steel non-threaded articles, unspecified. | 732690: Miscellaneous iron or steel articles. | 830120: Vehicle locks: key, combination, or electrically operated. | 830230: Base metal motor vehicle mounting and fittings. | 840731: Piston engines for vehicles, under 50cc capacity. | 840732: Reciprocating engines for 50-250cc vehicle propulsion. | 840733: Vehicle engines: reciprocating piston, 250-1000cc capacity. | 840734: Reciprocating piston engines for Chapter 87 vehicles. | 840820: Diesel engines for Chapter 87 vehicles. | 840890: Diesel engines for non-marine or vehicle use. | 840991: Engine parts for spark-ignition piston engines. | 840999: Parts for internal combustion piston engines. | 841330: Pumps for internal combustion piston engines. | 841391: Pump components and associated parts. | 841430: Refrigeration equipment compressors. | 841459: Fans: not elsewhere specified in item 8414.51 | 841582: Non-reversing, non-window/wall air conditioning units. | 841590: Air conditioning systems: temperature control and components. | 842123: Filtering machinery for internal combustion engines. | 842131: Engine intake air filters for machinery. | 842139: Gas purification machinery, excluding engine air filters. | 848210: Spherical bearings for rotational support. | 848220: Tapered roller bearings, including cone and assemblies. | 848240: Needle roller bearings are a type of bearing. | 848250: Cylindrical roller bearings (excluding heading 8482). | 848280: Bearings: components for rotational motion, not otherwise specified. | 848299: Bearing components, excluding balls, needles, and rollers. | 848310: Transmission, cam, and crank shafts and cranks. | 848350: Pulleys and flywheels, including blocks. | 848390: Transmission components for specific machinery or appliances. | 848410: Multi-layered metal gaskets and composite joints. | 848490: Assorted gaskets and joints, packaged for distribution. | 850132: DC motors, generators: 750W-75kW output. | 850520: Electromagnetic couplings, clutches, and brakes. | 850611: Primary manganese dioxide cells, under 300cm³. | 850612: Primary cells: <300cm³, mercuric oxide. | 850613: Primary silver oxide

cells, under 300cm³. | 850619: Primary cells and batteries, under 300cm³, per heading 8506. | 850620: Primary cells and batteries, over 300cm³ external volume. | 850690: Primary cells and batteries, including parts. | 850710: Lead-acid electric accumulators for piston engine starting. | 850720: Lead-acid electric accumulators, excluding engine starters. | 850730: Nickel-cadmium electric accumulators, including separators. | 850740: Nickel-iron electric accumulators, including separators. | 850780: Electric accumulators: n.e.s. including separators. | 850790: Parts of electric accumulators; not elsewhere specified. | 851110: Spark plugs for internal combustion engines. | 851120: Ignition/starting equipment for internal combustion engines. | 851130: Ignition and starting equipment for engines. | 851140: Ignition/starting equipment for internal combustion engines. | 851150: Ignition/starting equipment for internal combustion engines. | 851180: Ignition equipment for internal combustion engines. | 851190: Ignition/starting equipment for internal combustion engines. | 851220: Motor vehicle lighting and visual signalling equipment. | 852721: Radio receivers with sound recording/reproducing apparatus. | 852729: Radio receivers: external power source, no sound recording. | 853910: Sealed-beam lamp units. | 853921: Tungsten halogen filament lamps, excluding UV/IR. | 854150: Photovoltaic semiconductor devices: n.e.s. 8541 electrical apparatus. | 854430: Vehicle/aircraft/ship ignition and other wiring sets. | 870600: Chassis with engines for motor vehicles. | 870710: Motor vehicle bodies (including cabs) for heading 8703. | 870790: Motor vehicle bodies, including cabs. | 870810: Vehicle bumpers and parts for headings 8701-8705. | 870821: Vehicle body parts, including safety seat belts. | 870829: Vehicle body parts and accessories, excluding seat belts. | 870839: Vehicle braking systems: components and unmounted linings. | 870840: Automotive components: parts and gearboxes. | 870850: Vehicle driveline components: differential drive-axles and parts. | 870870: Vehicle road wheels and associated parts and accessories. | 870880: Vehicle suspension shock-absorber components. | 870891: Automotive components: parts and radiators. | 870892: Automotive exhaust components and parts. | 870893: Vehicle clutch components and parts | 870894: Automotive components: steering, columns, and parts | 870899: Vehicle parts and accessories, not elsewhere specified. | 902910: Various meters and counters for recording measurements. | 902920: Speed and tachometer indicators; stroboscopic meters. | 902990: Measuring instruments: parts, accessories, and speed indicators. | 940120: Motor vehicle seating: specialized types for various uses. | 940190: Seat components. | 960350: Brushes: machine, appliance, or vehicle components.

3. Parts and components

250410: Natural graphite: powder or flakes. | 250490: Natural graphite: non-powdered, non-flaked forms. | 250510: Natural silica and quartz sands, colored or not. | 250590: Natural sands, excluding silica, quartz, and metal-bearing. | 260111: Non-agglomerated iron ores and concentrates. | 260112: Agglomerated iron ores and concentrates. | 260120: Roasted iron pyrites | 260200: High-manganese ores and concentrates. | 260300: Concentrated copper ore. | 260400: Concentrated nickel ore minerals. | 260500: Cobalt ore and concentrate: industrial raw materials. | 260600: Aluminium ores and concentrates. | 290122: Unsaturated acyclic hydrocarbon: propene (propylene) | 320910: Aqueous acrylic/vinyl paints and varnishes. | 320990: Aqueous polymer-based paints and varnishes. | 381900: Hydraulic fluids: brake and transmission liquids. | 382000: Antifreeze and de-icing solutions. | 390210: Polypropylene: other olefin polymers in primary forms. | 390410: Primary vinyl chloride homopolymer. | 390422: Plasticized polyvinyl chloride: primary forms, mixed substances. | 390950: Primary form polyurethanes. | 391710: Plastics: artificial protein or cellulosic casings. | 391721: Rigid polyethylene pipes and tubes. | 391722: Rigid polypropylene plastic tubes, pipes, and hoses. | 391723: Rigid PVC tubes, pipes, and hoses. | 391729: Rigid plastic tubes, pipes, and hoses. | 391731: Flexible plastic tubes, pipes, hoses: 27.6MPa burst pressure. | 391732: Unreinforced plastic tubes, pipes, and hoses without fittings. | 391733: Fitted plastic tubes, pipes, and hoses. | 391739: Miscellaneous plastic tubes, pipes, and hoses. | 391740: Plastic fittings for tubes, pipes, and hoses. | 392020: Propylene polymer plastics: non-cellular, unreinforced, laminated films. | 400110: Natural rubber latex: primary forms or sheets. | 400121: Natural rubber, excluding latex, in smoked sheets. | 400122: Technically specified natural rubber, primary forms. | 400129: Natural rubber in primary or processed forms. | 400130: Natural gums: primary forms, plates, sheets, or strips. | 400211: Synthetic SBR and XSBR rubber in various forms. | 400219: Synthetic SBR/XSBR rubber in primary/sheet forms. | 400220: Synthetic butadiene rubber: primary forms or sheets. | 400231: Synthetic isobutene-isoprene rubber, primary forms or sheets. | 400239: Synthetic halo-isobutene-isoprene rubber: primary forms or sheets. | 400241: Synthetic chloroprene rubber: primary forms. | 400249: Chloroprene rubber: synthetic, primary forms or sheets. | 400251: Synthetic acrylonitrile-butadiene rubber (NBR) latex. | 400259: Synthetic acrylonitrile-butadiene rubber (NBR) in primary forms. | 400260: Synthetic isoprene rubber: primary forms or sheets. | 400270: Synthetic EPDM rubber: various forms and applications. | 400280: Rubber: natural and synthetic, primary or sheet forms. | 400291: Rubber: primary forms, sheets, or strips. | 400299: Primary rubber forms: sheets, plates, or strips. | 410110: Raw bovine hides, various weights. | 410121: Raw bovine hides: fresh/wet-salted, >14kg per skin. | 410122: Raw bovine hides and skins, fresh/wet-salted. | 410129: Raw bovine hides and skins, partial, wet-salted. | 410130: Raw bovine hides and skins, preserved. | 410140: Raw equine hides preserved for further processing. | 410410: Bovine leather: hairless, under 28 sq ft. | 410421: Vegetable-tanned bovine leather, raw or split. | 410422: Pre-tanned bovine leather, not further prepared. | 410429: Tanned bovine/equine leather, not further prepared. | 410431: Tanned bovine/equine leather, full/grain splits. | 410439: Hairless bovine/equine leather, excluding full/grain splits. | 520100: Unprocessed cotton fibers. | 590310: PVC-laminated textile fabrics. | 590320: Polyurethane-coated textile fabrics for various applications. | 590390: Coated textile fabrics, excluding specific polymers. | 720211: High-carbon ferro-manganese alloys. | 720219: Low-carbon ferro-manganese. | 720221: Ferro-silicon with over 55% silicon content. | 720229: Ferro-silicon with up to 55% silicon content. | 720230: Ferro-

silico-manganese: a type of ferro-alloy. | 720241: High-carbon ferro-chromium: a ferro-alloy. | 720249: Low-carbon ferro-chromium: a ferro-alloy. | 720250: Ferro-silico-chromium: a type of ferro-alloy. | 720260: Ferro-nickel, a type of ferro-alloy. | 720270: Ferro-molybdenum: a type of ferro-alloy. | 720280: Ferro-tungsten and ferro-silico-tungsten alloys. | 720291: Ferro-titanium and ferro-silico-titanium alloys | 720292: Ferro-vanadium: A type of ferro-alloy. | 720293: Ferro-niobium: a type of ferro-alloy. | 720299: Ferro-alloys not elsewhere specified in heading 7202. | 720310: Direct reduced iron: lumps, pellets, or similar forms. | 720390: High-purity ferrous products, various forms. | 720429: Alloy steel ferrous waste, excluding stainless steel. | 720610: Steel ingots: non-alloyed, excluding heading 7203. | 720690: Iron/non-alloy steel: primary forms (excluding ingots). | 720711: Low carbon, rectangular, semi-finished iron/steel products. | 720712: Semi-finished iron/steel: low carbon, rectangular cross-section. | 720719: Low-carbon non-alloy steel: semi-finished, non-rectangular products. | 720720: Carbon steel: semi-finished, 0.25% or more carbon. | 720824: Hot-rolled iron/steel coils, <3mm, width ≥600mm. | 720923: Cold-rolled non-alloy steel, 0.5-1mm thick. | 721031: Electrolytically zinc-coated, high-strength flat-rolled steel. | 721039: Zinc-coated, flat-rolled iron or non-alloy steel. | 722830: Hot-rolled alloy steel bars and rods. | 740200: Unrefined copper anodes for electrolytic refining. | 740311: Refined unwrought copper: cathodes and sections. | 740312: Refined, unwrought copper wire-bars. | 740313: Refined, unwrought copper billets. | 740319: Refined unwrought copper (excluding item 7403.1). | 740321: Unwrought copper-zinc base alloys (brass). | 740322: Unwrought copper-tin alloys (bronze) for professional use. | 740323: Unwrought copper-nickel or copper-nickel-zinc base alloys. | 740329: Copper: alloys not in 7403, excluding 7405. | 740911: Refined copper strip, >0.15mm thick, in coils. | 740919: Refined copper plates, sheets; not coiled, over 0.15mm. | 740921: Brass copper strip, over 0.15mm thick. | 740929: Brass plates, sheets: >0.15mm thick, not coiled. | 740931: Copper-tin strip, >0.15mm thick, coiled. | 740939: Thick copper-tin alloy plates and sheets, not coiled. | 740940: Copper: plates, sheets, strip of copper-nickel alloys. | 740990: Copper alloy plates, sheets, and strips. | 760110: Unwrought, unalloyed aluminium. | 760120: Unwrought and alloyed aluminium materials. | 760611: Rectangular unalloyed aluminium plates, sheets, and strips. | 760612: Thick, rectangular aluminium alloy sheets and strips. | 760691: Unalloyed aluminium plates, sheets, and strips. | 760692: Non-rectangular aluminium plates, sheets, and strips, over 0.2mm.

Appendix 03: Summary statistics

Variable	N	Mean	Std. Dev.	Min	Max
Panel A: Gravity Controls (Full Sample)	1,003,284				
Ln(Distance)	1,003,284	8.7	0.832	0	9.887
Contiguity (0/1)	1,003,284	0.018	0.133	0	1
Common Language (0/1)	1,003,284	0.348	0.476	0	1
Colonial Link, Origin (0/1)	1,003,284	0.006	0.076	0	1
Colonial Link, Dest. (0/1)	1,003,284	0.006	0.076	0	1
Common Colonizer (0/1)	1,003,284	0.082	0.274	0	1
Common Legal Origin (0/1)	1,003,284	0.063	0.244	0	1
Ln (GDP Exporter)	1,003,284	24.008	2.297	18.096	30.953
Ln (GDP Importer)	1,003,284	24.008	2.297	18.096	30.953
Ln (Population Exporter)	1,003,284	15.74	1.92	10.653	21.087
Ln (Population Importer)	1,003,284	15.74	1.92	10.653	21.087
Trade Policy Variable					
Trade Agreement (0/1)	1,003,284	0.183	0.387	0	1
Ln (Applied Tariff + 1) Section 17*	1,003,255	1.771	1.024	0	4.175
HS92 Dependent Variables (Full Sample, Millions USD) - [1995-2023]					
HS92 Total Trade	1,003,284	370.913	4,489.10	0	563,000.00
HS92 Section 17 Trade	1,003,284	39.34	732.138	0	126,000.00
HS92 HS87 Trade	1,003,284	30.59	652.413	0	123,000.00
HS92 Final Products	1,003,284	21.234	479.237	0	83,600.00
HS92 Parts & Components	1,003,284	24.325	476.014	0	92,000.00
HS92 Raw & Semi-Processed	1,003,284	13.836	302.417	0	109,000.00
HS17 EV Dependent Variables (Subsample, Millions USD) – [2017-2023]					
HS17 Total Trade	242,172	556.254	6,182.89	0	567,000.00
HS17 EV Total Trade	242,172	33.848	691.107	0	89,800.00
HS17 EV Raw Minerals	242,172	0.385	36.213	0	13,000.00
HS17 EV Processed Materials	242,172	2.45	41.718	0	6,451.40
HS17 EV Battery Materials	242,172	1.253	26.758	0	5,777.00
HS17 EV Core Components	242,172	24.319	603.439	0	83,300.00
HS17 EV Finished Vehicles	242,172	2.518	60.663	0	6,629.90
HS17 EV Infrastructure	242,172	2.924	61.948	0	7,969.10
Record Identifiers					
EX-Exporter, IM- Importer (186 ISO3)	AFG, AGO, ALB, ARE, ARG, ARM, ATG, AUS, AUT, AZE, BDI, BEL, BEN, BFA, BGD, BGR, BHR, BHS, BIH, BLR, BLZ, BOL, BRA, BRB, BRN, BTN, BWA, CAF, CAN, CHE, CHL, CHN, CIV, CMR, COD, COG, COL, COM, CPV, CRI, CUB, CYP, CZE, DEU, DJI, DMA, DNK, DOM, DZA, ECU, EGY, ERI, ESP, EST, ETH, FIN, FJI, FRA, FSM, GAB, GBR, GEO, GHA, GIN, GMB, GNB, GNQ, GRC, GRD, GTM, GUY, HKG, HND, HRV, HTI, HUN, IDN, IND, IRL, IRN, IRQ, ISL, ISR, ITA, JAM, JOR, JPN, KAZ, KEN, KGZ, KHM, KNA, KOR, KWT, LAO, LBN, LBR, LBY, LCA, LKA, LSO, LTU, LUX, LVA, MAC, MAR, MDA, MDG, MDV, MEX, MKD, MLI, MLT, MMR, MNE, MNG, MOZ, MRT, MUS, MWI, MYS, NAM, NER, NGA, NIC, NLD, NOR, NPL, NZL, OMN, PAK, PAN, PER, PHL, PNG, POL, PRK, PRT, PRY, PSE, QAT, ROU, RUS, RWA, SAU, SDN, SEN, SGP, SLB, SLE, SLV, SOM, SRB, SSD, STP, SUR, SVK, SVN, SWE, SWZ, SYC, SYR, TCD, TGO, THA, TJK, TKM, TLS, TON, TTO, TUN, TUR, TZA, UGA, UKR, URY, USA, UZB, VCT, VEN, VNM, VUT, YEM, ZAF, ZMB, ZWE				

Note: The analysis sample includes 186 unique exporters/importers selected based on data availability; observations with systematic missingness were dropped. To construct the balanced panel required for the TERGM analysis, missing GDP and Population covariates were imputed using both forward (last observation carried forward) and backward (next observation carried backward) filling. A similar forward-imputation method was applied to the tariff data, which were available only through 2021, to cover the full sample period ending in 2023. This tariff variable represents an aggregation of HS Section 17 (Vehicles, Aircraft, Vessels and Associated Transport Equipment). All trade values are reported in millions of U.S. Dollars (converted from their original units of thousands of USD). The tariff data was forward imputed since the data available up to 2021, but the sample covers up to 2023. Tariff data was aggregated for HS Section 17: (Vehicles, Aircraft, Vessels and Associated Transport Equipment.

=

Appendix 04: Network model estimation results

Variables	TERGM (1) HS92 Automotive	TERGM (2) HS92 Automotive	TERGM (3) HS Section 17	TERGM (4) HS92 Final Prod.	TERGM (5) HS92 Parts & Comp.	TERGM (6) HS92 Raw Mat.
Network Structure						
Edges (Intercept)	-24.09	-14.84	-14.76	-14.7	-16.56	-14.99
	[-24.92, -23.33]	*[-15.53, -14.13]*	*[-15.50, -14.07]*	*[-15.37, -14.00]*	*[-17.53, -15.46]*	*[-15.81, -14.20]*
Reciprocity (Mutual)	1.01	0.55	0.69	0.46	0.67	0.68
	[0.92, 1.10]	*[0.48, 0.64]*	*[0.62, 0.75]*	*[0.39, 0.54]*	*[0.57, 0.79]*	*[0.61, 0.78]*
Triadic Closure (GWESP)	0.92	0.63	0.9	0.46	0.88	0.62
	[0.67, 1.16]	*[0.46, 0.80]*	*[0.70, 1.08]*	*[0.33, 0.58]*	*[0.66, 1.10]*	*[0.49, 0.73]*
Dyadic Covariates (Gravity)						
Ln(Distance)	-0.89	-0.57	-0.54	-0.64	-0.47	-0.54
	[-0.91, -0.87]	*[-0.60, -0.54]*	*[-0.56, -0.51]*	*[-0.67, -0.60]*	*[-0.50, -0.44]*	*[-0.57, -0.50]*
Contiguity	0.74	0.32	0.33	0.38	0.31	0.2
	[0.67, 0.79]	*[0.24, 0.39]*	*[0.25, 0.40]*	*[0.30, 0.46]*	*[0.19, 0.40]*	*[0.12, 0.28]*
Common Language	0.3	0.19	0.19	0.16	0.17	0.16
	[0.27, 0.34]	*[0.16, 0.23]*	*[0.16, 0.22]*	*[0.12, 0.20]*	*[0.14, 0.21]*	*[0.13, 0.20]*
Colony (Origin)	0.92	0.69	0.73	0.51	0.59	0.79
	[0.72, 1.12]	*[0.50, 0.88]*	*[0.56, 0.94]*	*[0.34, 0.66]*	*[0.38, 0.83]*	*[0.59, 1.03]*
Colony (Destination)	0.6	0.27	0.3	0.29	0.33	-0.37
	[0.51, 0.69]	*[0.16, 0.38]*	*[0.18, 0.42]*	*[0.16, 0.40]*	*[0.19, 0.45]*	*[-0.53, -0.21]*
Common Colonizer	-0.23	-0.13	-0.14	-0.1	-0.02	-0.16
	[-0.27, -0.19]	[-0.18, -0.08]	[-0.19, -0.09]	[-0.16, -0.04]	[-0.10, 0.03]	[-0.25, -0.10]
Common Legal Origin	0.9	0.56	0.52	0.5	0.5	0.5
	[0.86, 0.95]	*[0.50, 0.62]*	*[0.46, 0.58]*	*[0.43, 0.58]*	*[0.43, 0.60]*	*[0.42, 0.59]*
Policy Variables						
Trade Agreement	0.29	0.19	0.17	0.18	0.26	0.25
	[0.27, 0.31]	*[0.16, 0.22]*	*[0.13, 0.20]*	*[0.15, 0.21]*	*[0.22, 0.30]*	*[0.23, 0.28]*
Ln(Applied Tariff)	-0.1	-0.06	-0.05	-0.07	0	0
	[-0.13, -0.07]	*[-0.09, -0.04]*	*[-0.07, -0.03]*	*[-0.09, -0.04]*	*[-0.02, 0.03]*	*[-0.02, 0.03]*
Nodal Covariates						
Ln(GDP Exporter) (Sender)	1.08	0.68	0.67	0.71	0.7	0.41
	[1.06, 1.11]	*[0.66, 0.70]*	*[0.65, 0.69]*	*[0.69, 0.73]*	*[0.68, 0.72]*	*[0.37, 0.44]*
Ln (GDP Importer) (Receiver)	0.16	0.08	0.09	0.04	0.14	0.24
	[0.13, 0.19]	*[0.05, 0.10]*	*[0.07, 0.11]*	*[0.02, 0.06]*	*[0.11, 0.17]*	*[0.21, 0.27]*
Ln (Population Exporter) (Sender)	-0.24	-0.15	-0.18	-0.14	-0.19	0.03
	[-0.28, -0.21]	*[-0.17, -0.13]*	*[-0.21, -0.16]*	*[-0.16, -0.12]*	*[-0.22, -0.16]*	*[-0.00, 0.06]*
Ln (Population Importer) (Receiver)	0.15	0.11	0.09	0.12	0.06	0.07
	[0.14, 0.16]	*[0.10, 0.12]*	*[0.08, 0.11]*	*[0.11, 0.14]*	*[0.05, 0.08]*	*[0.06, 0.09]*
Temporal Terms						
Memory (Stability)		1.66	1.58	1.71	1.71	1.87
		[1.63, 1.70]	*[1.55, 1.61]*	*[1.68, 1.74]*	*[1.69, 1.74]*	*[1.83, 1.91]*
Delayed Reciprocity		0.23	0.31	0.19	0.2	0.25
		[0.16, 0.28]	*[0.25, 0.36]*	*[0.09, 0.25]*	*[0.11, 0.27]*	*[0.16, 0.32]*

Variables	TERGM (8) HS17 EV Infrast.	TERGM (9) HS17 EV Raw Mi.	TERGM (10) EV Processed Mat.	TERGM (11) EV Battery Mat.	TERGM (12) EV Core Comp/	TERGM (13) EV Finished Veh.
Network Structure						
Edges (Intercept)	-21.23	-24.52	-19.79	-23.43	-20.01	-25.15
	[-22.42, -20.15]	*[-25.09, -23.82]*	*[-20.24, -19.30]*	*[-24.67, -22.42]*	*[-21.48, -18.64]*	*[-28.93, -22.47]*
Reciprocity (Mutual)	0.48	0.54	0.41	0.36	0.58	0.19
	[0.34, 0.61]	*[0.41, 0.63]*	*[0.16, 0.67]*	*[0.13, 0.55]*	*[0.42, 0.76]*	*[0.05, 0.32]*
Triadic Closure (GWESP)	0.34	0.5	0.48	0.22	-0.05	0.87
	[-0.00, 0.68]	*[0.39, 0.64]*	*[0.37, 0.59]*	*[0.15, 0.28]*	*[-0.39, 0.29]*	*[0.75, 0.98]*
Dyadic Covariates (Gravity)						
Ln(Distance)	-0.42	-0.46	-0.68	-0.6	-0.4	-0.71
	[-0.45, -0.40]	*[-0.51, -0.40]*	*[-0.78, -0.58]*	*[-0.63, -0.57]*	*[-0.42, -0.39]*	*[-0.76, -0.67]*
Contiguity	0.34	0.62	0.36	0.36	0.41	0.28
	[0.20, 0.51]	*[0.46, 0.75]*	*[0.27, 0.43]*	*[0.21, 0.52]*	*[0.20, 0.62]*	*[0.11, 0.46]*
Common Language	-0.01	0.13	0.23	0.24	0.11	-0.21
	[-0.05, 0.04]	*[0.07, 0.20]*	*[0.15, 0.32]*	*[0.20, 0.28]*	*[0.07, 0.15]*	*[-0.29, -0.09]*
Colony (Origin)	0.11	0.36	-0.07	0.17	0.15	-0.22
	[-0.11, 0.32]	*[0.07, 0.64]*	*[-0.38, 0.20]*	*[-0.07, 0.42]*	*[-0.16, 0.43]*	*[-0.39, -0.00]*
Colony (Destination)	-0.38	-0.79	-0.99	-0.77	-0.21	0.05
	[-0.52, -0.23]	*[-1.18, -0.42]*	*[-1.21, -0.86]*	*[-0.96, -0.54]*	*[-0.53, 0.09]*	*[-0.22, 0.33]*
Common Colonizer	-0.03	-0.18	-0.38	-0.04	-0.07	0.03
	[-0.14, 0.05]	*[-0.34, -0.03]*	*[-0.46, -0.26]*	*[-0.17, 0.08]*	*[-0.15, 0.02]*	*[-0.14, 0.22]*
Common Legal Origin	0.55	0.52	0.79	0.56	0.47	0.49
	[0.47, 0.62]	*[0.34, 0.71]*	*[0.62, 1.03]*	*[0.42, 0.70]*	*[0.41, 0.54]*	*[0.22, 0.69]*
Policy Variables						
Trade Agreement	0.32	0.27	0.27	0.4	0.27	0.36
	[0.26, 0.36]	*[0.18, 0.39]*	*[0.20, 0.36]*	*[0.34, 0.45]*	*[0.21, 0.34]*	*[0.22, 0.48]*
Ln(Applied Tariff)	-0.15	-0.12	-0.11	-0.1	-0.15	-0.21
	[-0.17, -0.12]	*[-0.15, -0.10]*	*[-0.14, -0.07]*	*[-0.14, -0.06]*	*[-0.19, -0.12]*	*[-0.30, -0.14]*
Nodal Covariates						
Ln(GDP Exporter) (Sender)	0.92	0.56	0.73	0.92	0.87	1.05
	[0.87, 0.95]	*[0.52, 0.59]*	*[0.69, 0.76]*	*[0.88, 0.96]*	*[0.83, 0.92]*	*[0.96, 1.17]*
Ln(GDP Importer) (Receiver)	0.23	0.45	0.28	0.26	0.22	0.38
	[0.23, 0.25]	*[0.43, 0.47]*	*[0.23, 0.33]*	*[0.23, 0.29]*	*[0.18, 0.25]*	*[0.32, 0.44]*
Ln(Population Exporter) (Sender)	-0.38	0	-0.17	-0.29	-0.36	-0.38
	[-0.39, -0.35]	*[-0.03, 0.03]*	*[-0.19, -0.15]*	*[-0.31, -0.27]*	*[-0.39, -0.33]*	*[-0.42, -0.34]*
Ln(Population Importer) (Receiver)	0.04	-0.01	0.04	0.09	0.06	-0.15
	[0.01, 0.06]	*[-0.04, 0.01]*	*[0.01, 0.08]*	*[0.07, 0.11]*	*[0.02, 0.10]*	*[-0.18, -0.12]*
Temporal Terms						
Persistence (Lagged Tie)	1.65	1.77	1.93	1.85	1.64	1.8
	[1.63, 1.66]	*[1.73, 1.82]*	*[1.90, 1.96]*	*[1.81, 1.88]*	*[1.60, 1.67]*	*[1.71, 1.87]*
Delayed Reciprocity	0.23	0	0.08	0.03	0.23	-0.01
	[0.09, 0.36]	*[-0.07, 0.10]*	*[-0.14, 0.29]*	*[-0.14, 0.24]*	*[0.07, 0.38]*	*[-0.11, 0.09]*

Appendix 05: Gravity model estimation results

Variable	PPML (1)	PPML (02)	PPML (3)	PPML (4)	PPML (5)	PPML (6)
	HS92 Automotive Trade (1995 - 23)			HS17 EV Trade (2017-2023)		
Dyadic Covariates (Gravity)						
Ln (Distance)	-0.327***	-0.404***	-	-0.508***	-0.263***	-
	(-18.82)	(-22.42)		(-13.96)	(-10.02)	
Contiguity	1.152***	0.864***	0.662	0.345***	0.830***	-
	-25.87	-29.19	-1.22	-3.62	-12.17	
Common Language	-0.322***	-0.157***	-	0.159*	-0.359***	-
	(-8.56)	(-5.98)		-2.15	(-4.23)	
Colony (Origin)	-0.582***	-0.269***	-	1.400***	-0.286*	-
	(-7.79)	(-4.42)		-6.66	(-2.19)	
Colony (Destination)	-1.263***	-0.115	-	-0.077	-0.465***	-
	(-14.85)	(-1.67)		(-0.43)	(-3.56)	
Common Colonizer	-0.772***	-0.557***	-	0.209	0.186	-
	(-11.41)	(-8.86)		-1.44	-1.31	
Policy Variables						
Trade Agreement	0.830***	0.653***	0.143**	1.029***	0.483***	0.049
	-23.85	-24.22	-2.58	-8.53	-6.08	-0.62
Ln(Applied Tariff)	-0.262***	-0.586***	-0.083**	-0.047	-0.230***	-0.253
	(-13.46)	(-31.45)	(-2.83)	(-0.94)	(-5.96)	(-1.75)
Nodal Covariates						
Ln (GDP Exporter)	1.086***	0.892***	-	0.845***	0.835*	-
	-72.08	-23.25		-35.56	-2.55	
Ln (GDP Importer)	0.847***	0.645***	-	0.912***	0.216	-
	-43.78	-15.17		-29.79	-0.68	
Ln (Pop-Exporter)	-0.173***	-0.39	-	0.140***	-3.132	-
	(-11.41)	(-1.75)		-4.27	(-1.68)	
Ln (Pop-Importer)	-0.012	-0.396***	-	-0.105**	1.837	-
	(-0.77)	(-4.50)		(-2.82)	-1.36	
Constant	-34.94***	-11.54**	14.75***	-33.38***	11.93	15.39***
	(-74.89)	(-2.86)	-82.72	(-38.41)	-0.26	-98.99
N Observations	1,003,255	1,003,255	746,304	242,165	242,165	138,810
Pseudo R^2	0.825	0.929	0.991	0.714	0.919	0.992
Fixed Effects						
ID (Direct Pair) FE	No	Yes	No	No	Yes	No
Exporter-Year FE	No	No	Yes	No	No	Yes
Importer-Year FE	No	No	Yes	No	No	Yes
Year + Partner FEs	No	Yes	No	No	Yes	No

Appendix 06: TERGM Goodness-of-Fit (GoF) diagnostics

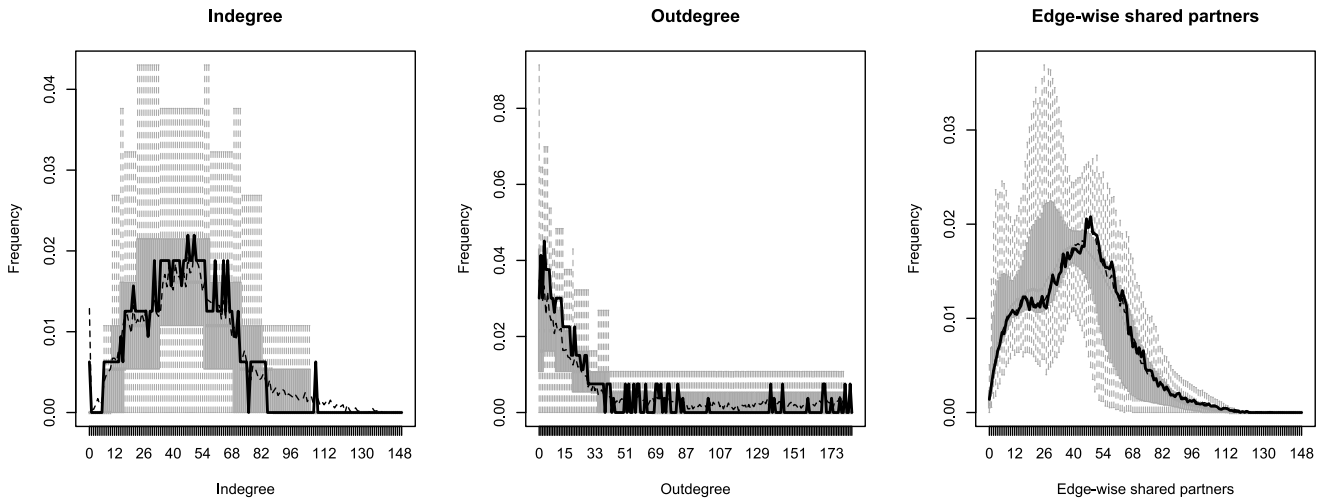

Note: To ensure the reliability of the main findings, a goodness-of-fit assessment was conducted, which indicates the TERGM provides a very good representation of the network's key structural properties. As shown in Figure 7, the observed distributions for edge-wise shared partners and indegree fall well within the simulation envelopes, demonstrating that the model successfully captures local transitivity and the distribution of incoming ties. A minor deviation is present in the outdegree distribution, where the model slightly underestimates the number of nodes with very few outgoing ties. This discrepancy likely points to unobserved heterogeneity, suggesting some nodes are inherently less active senders due to omitted variables. This issue is conceptually similar to the problem of multilateral resistance (MTR) in trade gravity models, where unobserved, time-invariant characteristics of exporters and importers can also bias estimates if not properly accounted for. Despite this minor point, these results collectively confirm the model is structurally well-calibrated for inference. The test is generated using built-in functions from the "btergm" package in R

Further enquiries

The University of Adelaide SA 5005 Australia
enquiries future.ask.adelaide.edu.au
phone +61 8 8313 7335
free-call 1800 407 527
web adelaide.edu.au
facebook facebook.com/uniofadelaide
X (twitter) twitter.com/uniofadelaide
tiktok tiktok.com/@uniofadelaide
instagram instagram.com/uniofadelaide
wechat UniversityOfAdelaide
weibo weibo.com/uniadelaide

Australian University Provider Number PRV12105
CRICOS Provider Number 00123M

December 2025. Job no. UA31717

Kaurna acknowledgement

We acknowledge and pay our respects to the Kaurna people, the original custodians of the Adelaide Plains and the land on which the University of Adelaide's campuses at North Terrace, Waite, and Roseworthy are built. We acknowledge the deep feelings of attachment and relationship of the Kaurna people to country and we respect and value their past, present and ongoing connection to the land and cultural beliefs. The University continues to develop respectful and reciprocal relationships with all Indigenous peoples in Australia, and with other Indigenous peoples throughout the world.